The Dissertation Committee for Cheasequah J. Blevins Certifies that this is the approved version of the following Dissertation:

EYELID CONDITIONING IN MICE REVEALS AN INTERACTION BETWEEN STRESS AND FAMILIAL ALZHEIMER'S DISEASE

Committee:

Boris V. Zemelman, Supervisor

Michael D. Mauk

Richard W. Aldrich

Kristen M. Harris

Robert O. Messing

EYELID CONDITIONING IN MICE REVEALS AN INTERACTION BETWEEN STRESS AND FAMILIAL ALZHEIMER'S DISEASE

by

Cheasequah J. Blevins

Dissertation

Presented to the Faculty of the Graduate School of

The University of Texas at Austin

in Partial Fulfillment

of the Requirements

for the Degree of

Doctor of Philosophy

The University of Texas at Austin

August 2019

Dedication

To James Larry Hammond, May 3, 1936 – January 18, 2019.

Acknowledgements

This dissertation would not have been possible without my mentors, lab mates, family and friends. I would like to thank Dr. Boris Zemelman and Dr. Michael Mauk for their support and mentorship. The rich perspectives I gained from learning from both of you were invaluable to the development of this dissertation and to my thinking as a scientist. Through all the challenges, I experienced a great deal of satisfaction piecing together the information, insight and skills necessary for this work.

I would like to thank Dr. Dan Johnston's laboratory for helping with the design and building of the behavioral equipment. To Dr. Richard Gray—I cannot thank you enough for introducing me to rig design and electronics. I had a lot of fun building equipment with your guidance, and I deeply appreciate all of the time and effort that you put into teaching and supporting me throughout.

I would like to thank my (almost) husband Eithan Kotkowski for his astonishing levels of encouragement and support. Specifically, thank you for helping to create beautiful figure artwork and for pushing me to improve in all aspects of life.

To my lab mates and my friends— Mariana Rodriguez-Santiago, Maya Kroth, Geoff Dilly, Eddie McCary, Eszter Kish, Neto Josh, Eric Hart, Stefanie Esmond and Matt Davis, Preeti Mehta, Madeleine Flexor Harrison, Devon Greer, Molly O'Gara, Aline Bridi, Eden Afework, Gabriela Garza and others: Thank you for making a friendly and helpful work environment. I have benefited greatly from working alongside each of you.

And for my friends, you have added the excitement and understanding that paints any endeavor bold and colorful with life. I'm so thankful to have shared this experience with you all!

Abstract

EYELID CONDITIONING IN MICE REVEALS AN INTERACTION BETWEEN STRESS AND FAMILIAL ALZHEIMER'S DISEASE

Cheasequah J. Blevins, Ph.D.

The University of Texas at Austin, 2019

Supervisor: Boris V. Zemelman

Detailed behavioral analysis can provide valuable information on the underlying neural machinery supporting learning. An associative learning model called eyelid conditioning is often used to study mechanisms and modulatory processes governing cerebellar motor learning. Here, I implemented this task in head-fixed mice, then probed learning in two mouse models of Alzheimer Disease. Triple-transgenic (3xTg) animals expressing mutant Amyloid Precursor Protein, Presenilin-1 (PS1) and tau proteins were conditioned at ages ranging from 3-16 months. Mutants displayed more rapid learning compared to controls at all ages tested. Additionally, 3xTg mice produced greater acoustic startle. Both behavioral phenotypes are consistent with heightened stress response. On the other hand, mice harboring a single knock-in PS1 mutation aged ~16 months learned the task poorly compared to littermate controls. Enhanced conditioning was observed in aged PS1 knock-in mice only after prolonged social isolation stress. Together, these support the existence of two distinct phenotypes in mutant mice: one that is related to heightened stress response, perhaps resulting from mutant transgene

overexpression (3xTg model), and one that is related to learning impairment, seen in the PS1 model.

Separately, I compared the effects of chronic and acute stress on conditioning in wild-type mice. Both chronic social isolation and acute shock enhanced learning, but with distinct characteristics. Isolation increased the rate of learning while shock did not; shock altered the timing of the motor response while isolation did not. To assess cerebellum-intrinsic phenotypes due to chronic stress, I replaced the peripheral CS with *in vivo* electrical stimulation of mossy fibers that supply CS information to the cerebellum. This experiment sought to distinguish cerebellum-intrinsic vs. extrinsic mechanisms driving rapid learning. I found that isolation-induced differences in learning rate disappeared when using a mossy fiber CS. This indicates that rapid learning observed after isolation is driven by inputs arriving via mossy fibers. Unexpectedly, stressed animals conditioned with stimulation displayed altered response timing, with longer latency to onset than controls. This result suggests that the cerebellum may adapt to long-term changes in input strength and thus offers a clue to why acute stress alters the motor response, but chronic stress does not.

Table of Contents

List of Figures

Chapter 1: Introduction

1.1 EYELID CONDITIONING AS A MODEL OF ASSOCIATIVE LEARNING

Classical conditioning has been used widely to model and study the associative learning process. Specifically, eyelid conditioning serves as a basic example of the "engram," the network of cells that hold a specific memory (Thompson, 2005). Extensive work during the 1970s – 2000s identified the cerebellum as the essential neuronal structure comprising the engram for eyelid conditioning, while regions such as the prefrontal cortex and amygdala were found to exert strong influence on the development and performance of this learned behavior under sub-optimal cue conditions.

Advances in mouse genetics have motivated an interest in expanding these foundational findings to include mechanistic studies of learning and memory at the genetic and biochemical level (Wang et al, 2017; Ezra-Nevo et al, 2018a). Due to the strong influence of structures associated with emotionality and cognition, eyelid conditioning has been used to examine and define functional abnormalities in humans with brain disorders and diseases such as autism (Sears et al, 1994; Welsh et al 2016), Alzheimer's Disease (Woodruff-Pak et al., 1990), post-traumatic stress disorder (Burriss et al., 2007; Myers et al., 2012) and schizophrenia (Forsythe et al., 2012), as well as in animal models of these brain disorders and diseases (Koekkoek et al, 2005; Justice et al., 2015). The purpose of this dissertation is to use these foundational ideas as a platform on which to dissect the behavioral phenotypes in two mouse models of Alzheimer's Disease, one expressing multiple familial mutations (3xTg) and one having only one mutation

(PS1). By testing both the 3xTg (which expresses three mutations, including PS1) to a mouse model harboring only a PS1 mutation, the contribution of the PS1 mutation to changes in learning and memory can be isolated.

Procedure

Eyelid conditioning is a multi-trial, incremental associative learning paradigm wherein a cue of neutral valence that does not elicit a behavioral response, usually a light or a tone, is paired in tight temporal succession with an eyeblink-eliciting unconditioned stimulus (US), such as a corneal air-puff or direct electrical stimulation of the orbicularis oculi muscle. After many trials, the animal learns to make a conditioned response (CR) eyelid closure to the previously neutral conditioned stimulus (CS). The temporal succession of the two cues, known as inter-stimulus interval (ISI), and the intensity of both the CS and US dictate the difficulty of the task.

Temporal properties of the CR reflect CS-intensity and cerebellar computations

Unlike a simple reflex, the CR displays temporal characteristics that match the temporal succession of the CS and US (Figure 1.1C-D). Response timing is an important aspect of cerebellar learning that is primarily accomplished by the cerebellar cortex (Garcia & Mauk, 1998; Kalmbach et al., 2010) and is a hallmark of cerebellar learning. Response timing can also be affected by the intensity of the CS input to the cerebellum, making it an important measure when investigating the influence of extracerebellar structures on eyelid conditioning as will be done in this dissertation.

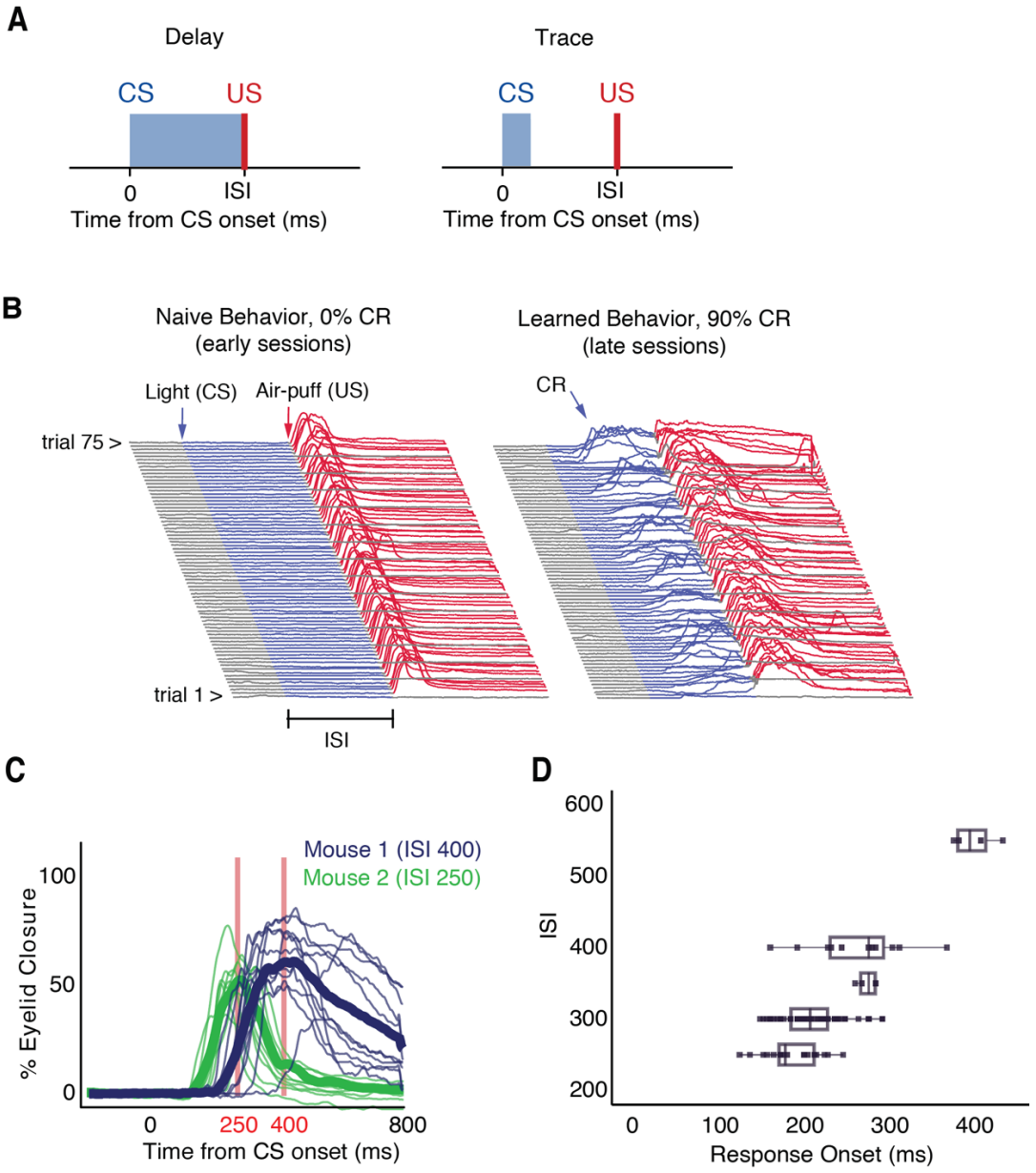

Figure 1.1: Behavioral Properties of Eyelid Conditioning.

A. Configuration of cue presentation for delay and trace conditioning. **B.** Example data capturing learning dynamics across behavioral sessions. Each line represents eyelid position for a single trial. **C-D.** Cerebellar motor learning displays adaptive timing. **C.** Single trials (light lines) and heavy lines (average) are plotted for two animals trained at different ISIs. **D.** Response onset (timing) is plotted against training ISI for animals trained at different ISIs. Each datapoint represents average CR timing per animal.

1.2 NEURAL CIRCUITRY SUPPORTING EYELID CONDITIONING

CS Pathway

Figure 1.2 depicts the relevant neural circuitry for eyelid conditioning. Information about the CS is processed both cortically (Siegel et al, 2015) and sub-cortically (Halverson et al., 2010) and then transmitted to the cerebellum though a large white matter tract known as the mossy fibers. The mossy fibers branch upon entering the cerebellum. One branch is sent to innervate granule cells and interneurons in the cerebellar cortex and the other is sent to the deep cerebellar nuclei. Most mossy fibers arise in the pons, a brainstem structure that receives a broad sampling of sensory information from the cortex. Also entering the cerebellum via the mossy fibers are brainstem sources of afferents from the locus coeruleus, raphe nuclei, vestibular nuclei and other sensorimotor nuclei throughout the reticular formation (Errico & Barmack, 1993; Bishop GA, 1998; Kimoto et al., 1981). Although the function of these mossy fiber inputs is poorly understood in the context of cerebellar motor learning, they may be involved in CS cue modulation due to extensive expression of neuropeptides such as norepinephrine (locus coeruleus) and corticotropin-releasing factor (raphe nuclei, vestibular nuclei and various sensorimotor nuclei) (Errico & Barmack, 1993; Bishop GA, 1998; Pomrenze et al., 2015).

US Pathway

Information about the US enters the brain by way of the cornea (in the case of air-puff US) and relays this information to the trigeminal nerve, which in turn relays information to the inferior olive (IO). The inferior olive is a brainstem nucleus composed of small, electrically

coupled neurons that send their sole output as climbing fibers to the cerebellum. Similar to the mossy fibers, climbing fibers enter the cerebellum and branch, sending one branch to the deep cerebellar nuclei (DCN) while the other branch sends fibers that synapse extensively onto the dendritic tree of only one Purkinje cell in the cerebellar cortex. Through complex cerebellar plasticity triggered by paired CS-US presentation, the inhibitory Purkinje cells acquire a learned pause in their tonic firing, momentarily disinhibiting cerebellar output neurons in the DCN. Output neurons from the DCN project to premotor areas in the brainstem, ultimately resulting in a learned eyelid movement with temporal characteristics reflecting the ISI used in training.

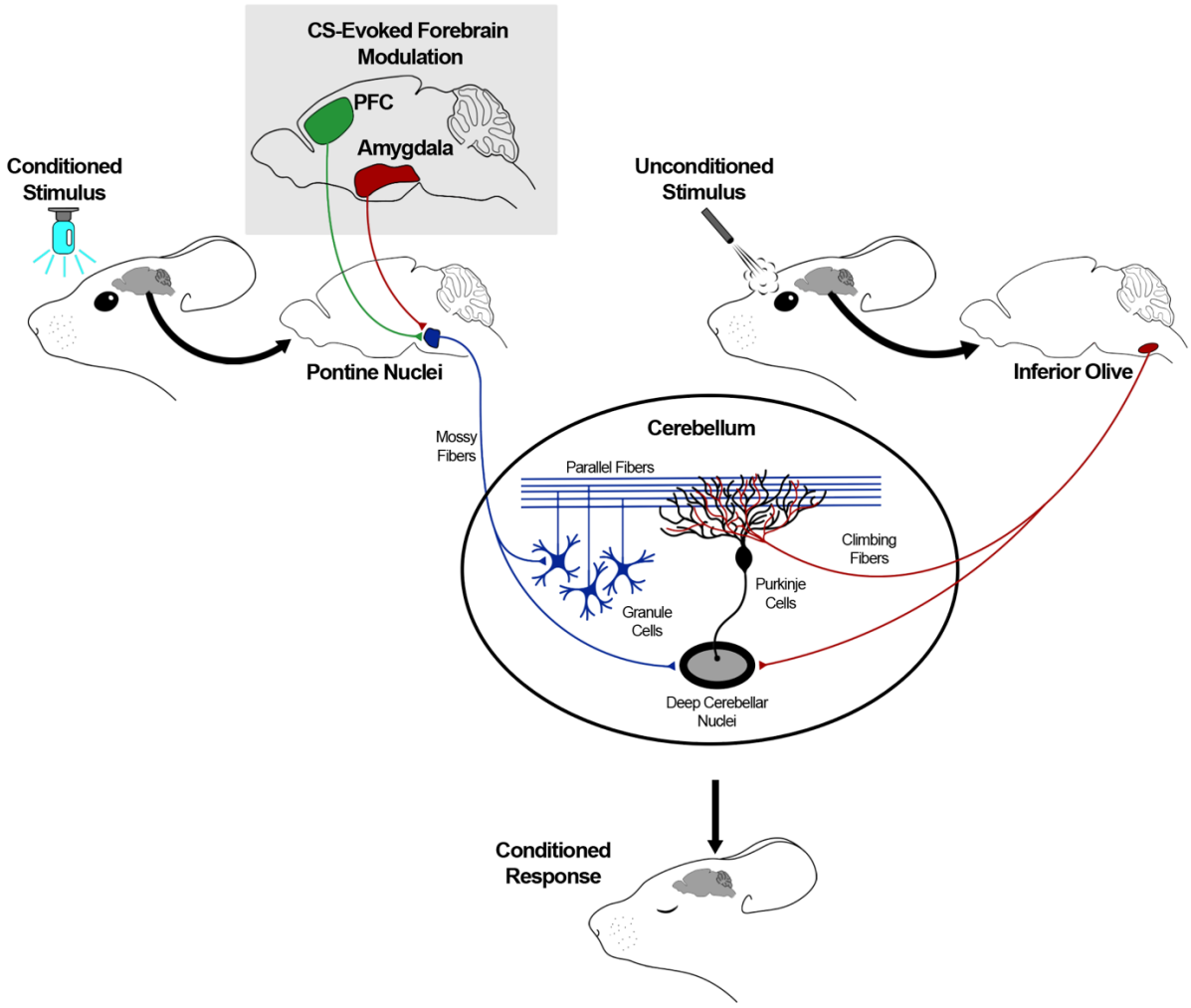

Figure 1.2: Neural circuitry important for eyelid conditioning

Inhibitory connection (Purkinje cell to DCN) indicated by filled circle at axon terminal, and excitatory connections indicated by triangles. A neutral conditioned stimulus (CS, depicted as a blue light) is paired hundreds of times with a blink-evoking unconditioned stimulus (US, corneal air-puff). CS information processed in the forebrain, including the hippocampus and prefrontal cortex, enters the cerebellum by way of the mossy fibers originating primarily in the basilar pontine nucleus, but also in other brainstem nuclei. Amygdala exerts modulatory influence on CS information entering the cerebellum, likely through direct projection from the central amygdala to the basilar pontine nucleus. US information arrives to the cerebellum by climbing fibers originating in the inferior olive. CS-US information converge in the cerebellar cortex and deep cerebellar nuclei, the two essential sites of plasticity for eyelid conditioning, and signals dictating the learned eyelid movement leave the cerebellum from DCN efferent projections to premotor areas.

1.3. FOREBRAIN INVOLVEMENT IN EYELID CONDITIONING

Because the essential circuitry for eyelid conditioning is in the cerebellum, it has proven to be an invaluable tool for probing mechanisms of cerebellar motor learning. At its most basic level, eyelid conditioning engages the cerebellum directly through CS and US inputs from the mossy and climbing fiber afferents, respectively, as described in Figure 1.2. Indeed, direct electrical stimulation of the mossy fibers that overlaps in time with direct simulation of the inferior olive is sufficient to induce a learned eyelid response (Mauk et al., 1986; Steinmetz et al., 1989).

However, under sub-optimal conditions—when CS cue intensity is weak (weak-CS conditioning) or when the CS and US are separated by a temporal gap (trace conditioning), subjects have a hard time learning. Both types of conditioning require more trials to learn and produce fewer CRs at asymptotic performance than delay conditioning with strong conditioning stimuli. Successful learning in these cases requires forebrain structures including the mPFC and the amygdala, as lesions to either of these structures prevents or dramatically slows learning under sub-optimal cue conditions.

Amygdala potentiates CS-evoked responses in the cerebellum

Infusions of the $GABA_A$ agonist muscimol into the central amygdala (CeA) during eyelid conditioning prevents acquisition (Farley et al., 2016) and expression (Siegel et al., 2015) of the conditioned response. Unit recordings in the DCN, the structure that drives learned motor responses, showed greatly reduced CS-evoked activity during CeA inactivation (Farley et al., 2016). Further, enhanced conditioning is observed when amygdala excitability is increased by

stress (Shors et al., 1992, Weiss et al., 2005). Together, these studies show that the amygdala is important for the acquisition and expression of eyelid conditioning in rodents, likely through its function in strengthening CS-related signals arriving to the cerebellum (Fig. 1.2).

mPFC is required for trace eyelid conditioning

Trace conditioning requires sensory-driven input from the PFC (Kalmbach et al., 2009; Siegel et al., 2015), thalamus (Halverson et al., 2010), and (in rodents at least) the amygdala (Blackenship et al., 2005; Siegel et al., 2015, Farley et al., 2016). These CS-evoked signals arrive to the cerebellum through converging projections to the pons, as in Fig. 1.2 (Kalmbach et al., 2009; Siegel et al., 2015). Due to the strong modulatory influence of forebrain structures, trace conditioning has been used widely as a systems-level model of higher-order learning, invoking concepts such as working memory (Kalmbach et al., 2009) and awareness (Manns et al., 2000).

Learning likely reflects integration of all forebrain inputs

One possibility is that there are at least two mechanisms by which the forebrain assists in cerebellar motor learning. First, when cue sensitivity is low, the amygdala may predominately contribute to learning through potentiation of CS-evoked responses (Freeman et al., 2018). Second, when there is a temporal gap between the two stimuli, the forebrain may contribute by providing persistent activity from the PFC projection to the pons (Kalmbach et al., 2009; Kalmbach et al 2010).

Of course, these two mechanisms are not mutually exclusive. It is important to keep in mind that these two mechanisms can contribute simultaneously, and any learned behavioral

output from an intact brain should be considered a combination of both. For example, optogenetic silencing of mPFC terminals to the basilar pontine nucleus dramatically slow learning in weak-CS delay conditioning (Wu et al., 2017), while muscimol silencing of the amygdala prevents expression of behavioral CRs in trace conditioning (Siegel et al., 2015). Thus, persistent activity may contribute to learning during dim-cue delay conditioning, and the amygdala may potentiate PFC persistent activity during trace conditioning.

Direct evidence testing the hypothesis of two separate mechanisms of forebrain involvement does not currently exist. However, indirect anatomical and inactivation evidence supports the idea. The "working memory" PFC projection to the pons projects predominately to the lateral basilar pontine nucleus (Kalmbach et al., 2009; Siegel et al., 2015), and inactivation selectively of the lateral basilar pontine nucleus abolishes trace but not delay conditioning (Kalmbach et al., 2009). On the other hand, the amygdala projection to the basilar pontine nucleus terminates much more extensively in the basilar pontine nucleus (Siegel et al., 2015), covering areas of the lateral and medial regions. Thus, the amygdala projection is suited to potentiate CS signals coming to the pons from a variety of sources, while the PFC projection arrives in a specific anatomical location and may have a completely independent function.

1.4 GENETICS OF ALZHEIMER DISEASE

In a small subset of AD patients, about 5% of all cases (Tanzi et al., 2012), causal mutations in *Presenilin-1 (PS1), Presenilin-2, and β-Amyloid Precursor Protein (APP)* were identified in the 1990s (Goate et al., 1991; Clark et al., 1995; Sherrington et al., 1996). Additional mutations are still being discovered today (Shen et al., 2019), suggesting that a larger

proportion of AD cases may in fact be caused by yet unknown mutations. Inheritance of any of these mutations causes, with 100% penetrance, an aggressive form AD, with cognitive symptoms appearing before the age of 65 and as early as the late twenties, depending on the specific mutation in question. Mutations in PS1 causes the most severe form of the disease, with cognitive decline often beginning in the 30s and 40s, while APP and PS2 mutations typically cause less aggressive pathology (Ryman et al., 2014).

Presenilin (either 1 or 2) joins three other proteins, nicastrin, anterior pharynx-defective 1 (APH-1) and presenilin enhancer 2 (PEN-2) to form the gamma-secretase complex, a membrane associated protease found in many locations within the cell, including on both sides of the synapse (Schedin-Weiss et al., 2016) and on the endoplasmic reticulum (Area-Gomez et al., 2009). Gamma secretase endogenously cleaves several type I transmembrane signaling proteins, including Notch, a signaling protein crucial for cell-fate decisions during development, and N-Cadherin, involved in neural circuit assembly (Jontes, 2018). Importantly, gamma-secretase is responsible for the cleavage of APP, a process that releases neuro-toxic amyloid-β protein into the extracellular space. In addition to aggregating into the characteristic amyloid-β plaques, the soluble form of amyloid-β protein elicits neuronal hyperactivity (Busche et al., 2012), perhaps by direct activation of g-protein coupled receptors such as corticotropin-releasing factor type-1 receptor (CRF-R1) (Justice et al., 2015; Park et al., 2015).

PS1 can participate in neuronal activity and plasticity by multiple mechanisms. One study demonstrated the importance of presynaptic PS1 for calcium-dependent neurotransmitter release at the synapse by genetic deletion of PS1 in hippocampal CA3 cells (Zhang et al., 2009). Following genetic deletion, both long-term and short-term plasticity were impaired following

theta burst stimulation of the Schaffer collaterals, while genetic deletion post-synaptically in the CA1 neurons did not affect plasticity. PS1 is additionally involved in Ip3-induced calcium release from the endoplasmic reticulum (Stutzmann et al., 2004), where the protein has also been localized. Finally, synaptotagmin, a protein essential for calcium-dependent neurotransmitter release, was identified as a synaptic binding partner of PS1 (Kuzuya et al., 2016). Thus, there are several distinct mechanisms by which PS1 can affect neuronal activity and plasticity.

More than 175 mouse models have been developed since the mid 1990s (alzforum.org) to model AD, and most are based on overexpression of one or more causal mutations in APP, PS1 and PS2. Because early theories of AD implicated amyloid-β protein as the primary disease driver, the models were generally developed to maximize amyloid-β production. While most carry transgenes that over-express multiple mutations, more recent models have dialed back the intensity, choosing to model the disease by knock-in of a single mutant (Guo et al, 2012; Justice et al., 2015). One reason for the push to simplify was that the multiple-transgene models often display erratic behavioral profiles not mirrored in the human population. Some of these behaviors include high levels of anxiety, enhanced associative learning, and larger acoustic startle reflex, all of which have been linked to a heightened stress response (Justice et al., 2015).

1.6 BEHAVIORAL RIG DESIGN

Here, I describe an Arduino-controlled mouse eyelid conditioning rig based on previously published designs (Heiney et al., 2014, Desai et al., 2015; Siegel et al., 2015).

Cue Delivery

Neuroscience research typically requires both hardware and software that provides an interface between stimulus delivery and data acquisition. Historically, this need has been satisfied by expensive data acquisition systems such as by InstruTECH. While more complex control requirements, such as electrophysiological experiments requiring reliable nanosecond precision, may still necessitate traditional data acquisition and stimulus control systems, do-it-yourself hobbyist tools such as Arudino and Raspberry Pi have proven themselves as exceptional alternatives when microsecond precision is sufficient, as in the current purpose of behavior analysis in this dissertation (D'Ausilio A, 2012; Desai et al., 2015).

I have implemented a system of cue delivery and data acquisition that relies on an Arduino Due microcontroller board to coordinate delivery of the conditioned and unconditioned stimuli, as well as to trigger the high-speed camera during each trial. In addition to controlling the timing of stimuli, the Arduino board monitored and controlled the air-puff pressure by implementing a proportional-integral-derivative (PID) algorithm acting on a proportional valve. The air puff US was delivered using a sawed and blunted 28-gauge stainless steel needle adhered to a cannula and positioned 2– 4 mm lateral to the right eye (Fig. 2.1). Each training chamber also included a small speaker (Adafruit product ID 1891) through which white noise played on loop from a custom designed sound board (Adafruit audio FX mini sound board, Product ID 2342) and amplifier system (Adafruit Mono 2.5W Class D Audio Amplifier PAM8302, product ID 2130) that measured 55 dB at site of the mouse head.

The Arduino board was further responsible for generating a sine wave that plays directly through a speaker-amplifier system to provide a second CS for eyelid conditioning and to probe

acoustic startle responses. Tones were generated by programming an approximate sine wave into an Arduino microcontroller and then running the wave through an amplifier-speaker system (Adafruit Mono 2.5W Class D Audio Amplifier PAM8302, product number 2130; Mono Enclosed Speaker: 3W 4 Ohm, product number 3551).

Finally, in experiments that used direct electrical stimulation as a conditioned stimulus, the Arduino board was responsible for generating the appropriate stimulus parameters (Kalmbach et al., 2010) to the stimulus isolator box (World Precision Instruments) which generated the cathodal delivered to the brain.

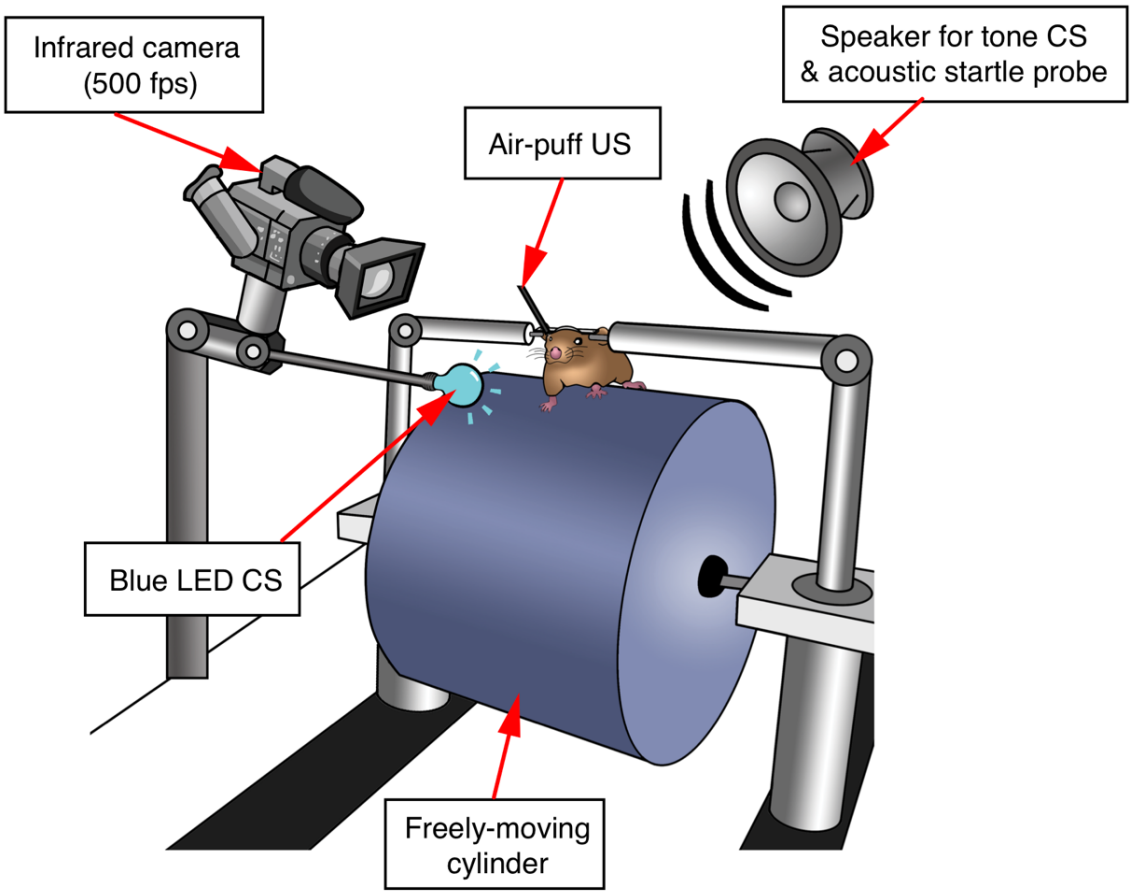

Figure 1.3: Eyelid conditioning in head-fixed mice.

Mice are secured atop a freely-moving cylinder during all eyelid conditioning sessions. A 500-fps infrared video of the eye is recorded during stimulus presentation to record learned eyelid movements. Not depicted here is an infrared LED panel, positioned behind the blue CS LED (away from the mouse) that remains on during the entire behavior session and serves to illuminate the eye. All behavior sessions took place in the dark.

Eyelid monitoring

To record eyelid movements at high spatial- and temporal precision, 500 fps high-speed videography (Allied Vision Technologies GE680 gigabit Ethernet camera) was used. To extract eyelid traces, raw videos were analyzed with un-published, custom software written in Igor Pro (WaveMetrics, Lake Oswego, OR, USA). As depicted in Figure 1.4, video pixels underwent thresholding such that all pixels were either black (representing the mouse eye) or white (representing the fur around the eye). White pixels within a user-defined region of interest were summed at each frame, and the summed values over a 1.2 s window were normalized to the [0,1] range, with 0 representing the value in the first frame (eye fully open) and 1 representing all white pixels (eye fully closed). These values were then written to a text file for further processing.

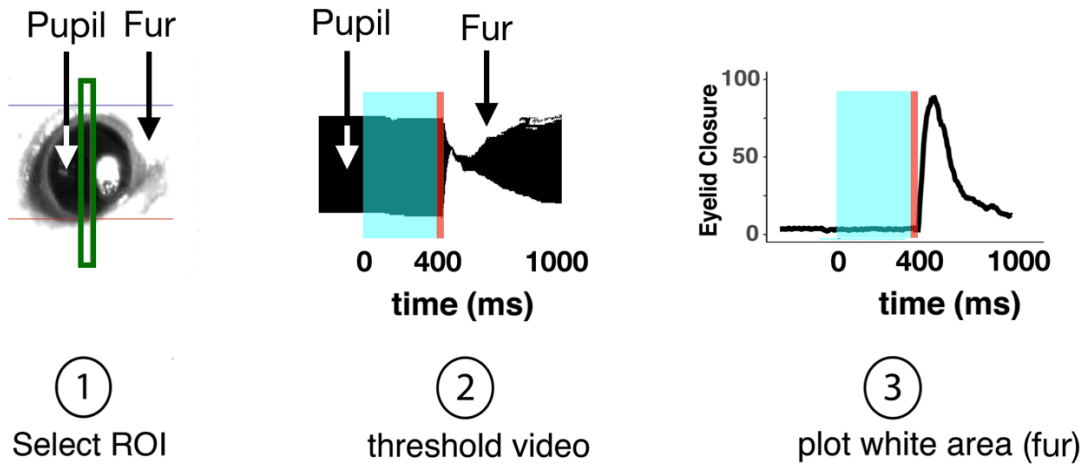

Figure 1.4: High-speed video analysis of eyelid movement

Schematic of video processing. An ROI (green) was drawn for each animal per behavior session at the widest part of the fully opened eye. Video data within the ROI was thresholded to black or white on each frame across the video. Finally, the fraction of white area (representing the fur around the eye) at each frame was computed and plotted across time. Shaded blue region represents CS presentation and red shaded region represents US presentation.

1.7 DATA PROCESSING AND DERIVATION OF MEASUREMENTS

The sole type of data analyzed in this thesis are time-series "eyelid traces" derived from videography data and representing the fraction of eyelid closure over time (Heiney et al., 2014, Siegel et al., 2015). After recording the reduced eyelid traces to a text file, an R script (R Core Team, 2019) was written to assess data integrity, excluding traces whose baseline noise standard deviation during the first 200 ms of the trace exceeded 0.025. Finally, the following events were extracted from the traces: presence or absence of conditioned response, latency to conditioned response onset, and magnitude of conditioned response, and trials to learning onset. Figure 2.3 depicts the anatomy of an eyelid trace and summarizes the measurements relevant to this thesis and how they are derived.

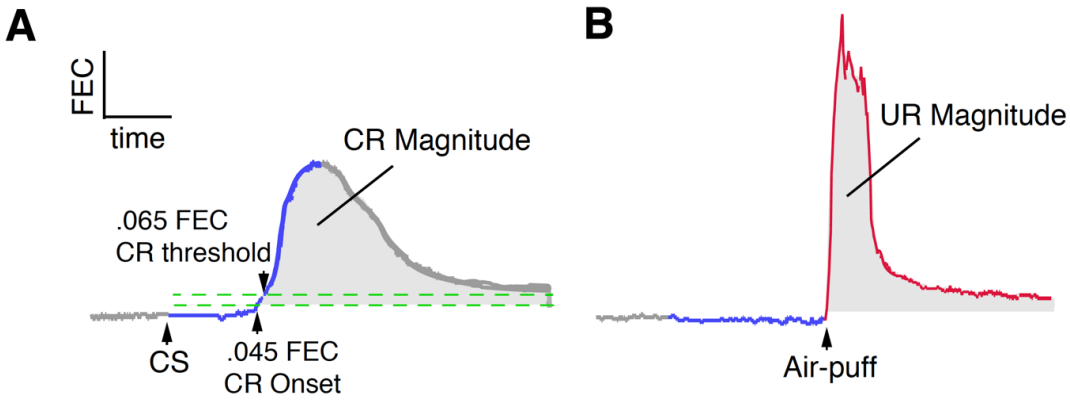

Figure 1.5: Components of an eyelid trace.

A. representative eyelid trace from a CS-alone probe trial. The top dotted green line represents the threshold for classifying a trial as a CR. Once a trial is classified as a CR, the time at which the trace crosses the bottom green dotted line is recorded as the response onset. The CR magnitude is measured as the summed FEC values at each frame under the CR (shaded gray). **B.** Unconditioned response (UR) magnitude measures the mouse's response to the air-puff (red) and is a measure of US sensitivity.

A peak-finding algorithm was used to find the maximum value of a trace above a pre-set threshold. If any peaks were found during a 1000 ms window after CS onset, then the trial was classified as a CR. Previous publications using videography to assess mouse eyelid conditioning used 10% eyelid closure threshold for a classification as CR (Heiney et al., 2014; Siegel et al., 2015). While a standard threshold for rabbit eyelid conditioning is 5%, the discrepancy is likely due to the smaller size of the mouse eye compared to the rabbit eye and thus to the higher level of noise associated with measuring eyelid movements. Further, I chose 6.5% as the classification threshold for CR, an empirical choice that results in < 1% false positives as measured by analysis of stimulus-free trials.

Response properties of learned eyelid movements are of biological importance because they are driven directly by learned cerebellar output (Heiney et al., 2014) and reflect properties of cerebellar learning. Due to the nature of the eyelid trace data, in which response peak is usually ambiguous, I chose response onset to assess timing (Fig. 2.3A). To measure the size of the response, two possibilities exist, response amplitude (maximum closure achieved during a CR) and response magnitude (area under the CR) magnitude. Because of the larger range and higher variability of magnitude measurements, I chose response magnitude to measure the size of the response (Fig 2.3A).

Custom R script was used to create visual statistical summaries of the responses. To create a within-animal visual summary, summary CR traces $j = 1, 2,..., N$ were aligned temporally across the $k = 1, 2,... 600$ frames represented by the trace (1.2 s x 500 fps = 600 frames). At each k, the distribution of the median value of j was derived using bootstrap, and the central 95% confidence interval was plotted (Fig. 1.6). To create within-group visual summaries,

traces from each animal were reduced to a median trace. Animal-representative median traces were then analyzed in the same way as described for per-animal summaries.

Because responses change over time with learning, it is important to control for learning when making comparisons of response onset and magnitude. For example, if the median response measure was recorded for an animal that learned poorly and was compared to the median response of an animal that learned very well (and thus made many more responses), then the better learner would have a higher median. To control for learning when measuring response properties, I use only a subset of CRs made by each animal to compare response properties. Usually, this was the 51-100th conditioned response made by each animal. In experiments where poor learning was observed overall (Chapter 3 only), I lower this number to 31-80th. If an animal did not make at least 100 (or 80) responses, then they were excluded from measurement of response properties.

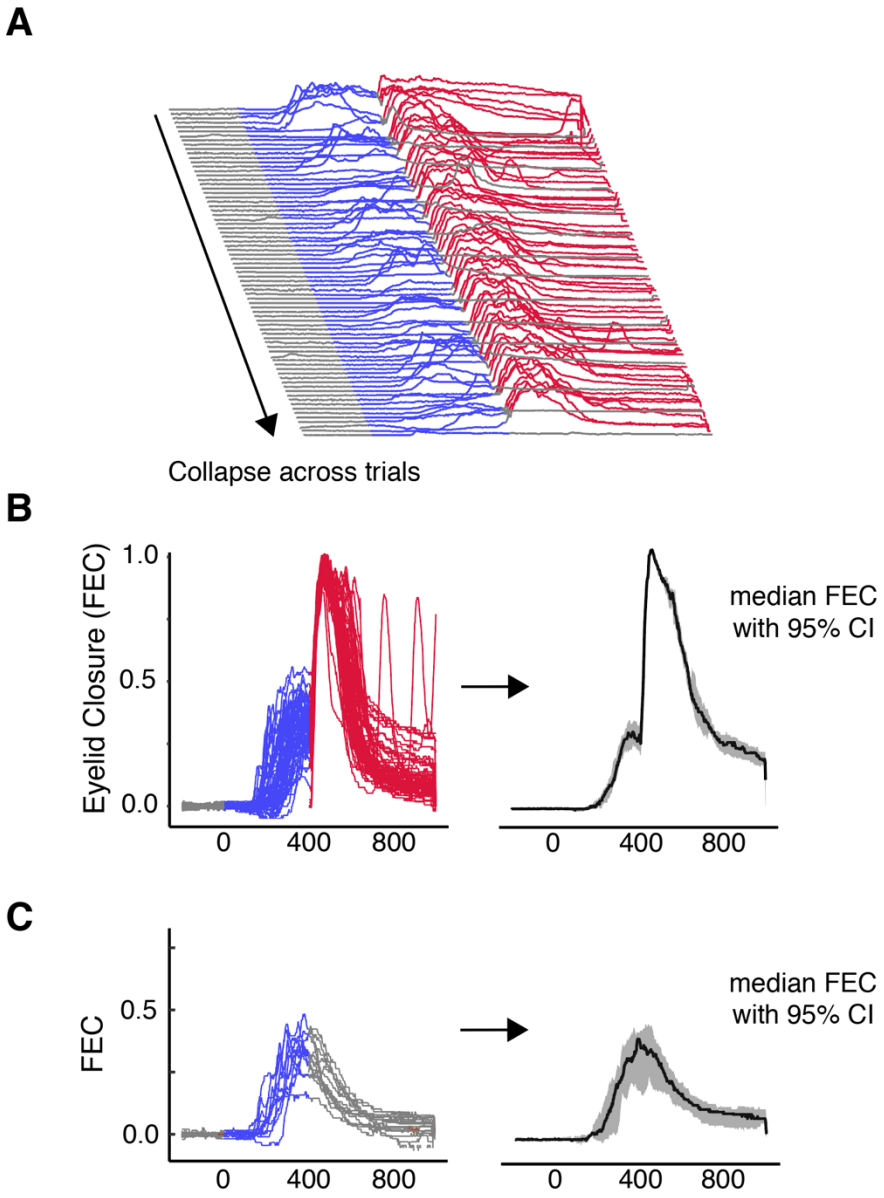

Figure 1.6: Derivation of statistical summaries of eyelid traces

A. Individual trials are collapsed across CR trials and non-CR trials are excluded. Paired (B) and CS-only probe trials are aligned across time and median point at each frame is plotted inside of a shaded 95% CI derived using bootstrap.

1.8 STATISTICAL PROCEDURES

It is well-established that sex-differences exist in most behaviors commonly studied in laboratory animals. Baseline behaviors between male and females are often different and experimental manipulations can have sex-dependent outcomes. Thus, it is common practice to exclude either male or female from a study when sex differences are not the main focus. However, not all results can be generalized to both sexes and excluding one or the other creates a blind spot in our understanding of biological phenomena. Because I have no *a priori* justification to exclude one sex, I have chosen to include both as I was not studying sex-differences *per-se*. The experiments were therefore not designed to detect statistically significant results between male and female subgroups -- i.e., there were not enough males and females within each subgroup for adequately powered inference tests for each sex. Low sample size and normality of residual violations additionally preclude a regression approach for controlling for sex.

To account for sex as a covariate, I used restricted randomization permutation testing (Edington, 2007). This technique resembles permutation testing, except that treatment randomization is restricted to male and female sub-groups. The advantage of this approach is two-fold. First, when response variables exhibit different baseline values for males and females, restricted randomization results in more powerful inference testing. Second, when the number of males and females are not perfectly balanced across groups, restricted randomization controls for false positives that may result from comparing groups with unbalanced covariates.

As an example, consider the social isolation experiment from Chapter 4. There were four subgroups to sample: Female-Stress (n = 6), Female-Control (n = 6), Male-Stress (n = 8), Male-Control (n = 8). There are two blocks randomization: Female (n = 12) and Male (n = 16). Finally,

there were two groups to compare: Stress (n = 14) and Control (n = 14). To simulate a test statistic, treatment labels were randomized within female and male subgroups, dependent on how many male and female animals were in the original data. In this case, both treatment groups had 14 animals, with 6 females and 8 males in each. Finally, the test statistic computed from the original data was compared to the distribution of statistics calculated from permutation testing. The proportion of simulated statistics with a value greater than the statistic calculated from the original data is the p-value.

Permutation tests are computationally expensive, as they require computing all possible permutations of the data (or at least a very large, random subset). For example, in the experiment outlined above, there are $\binom{12}{6} \times \binom{16}{8} = 40{,}116{,}600$ possible permutations to consider. Fortunately, the R-package "coin" can approximate results from Kruskal-Wallis rank test based on stratified data (Hothorn et al., 2008). To verify that the commands from the coin package produced similar results as the more computationally exhaustive method of direct permutation testing, I computed several p-values based on restricted subsample randomization testing (100,000 permutations) and verified that they produced values very similar to those computed by "coin".

This technique can be used to handle experimental variability across experiments. Learning rate can be considerably affected by non-experimental factors such as housing conditions and genetic variability, meaning that combining data from separate experiments, even when all controllable parameters remain equal, can present problems. Collecting enough data for a study in one experiment is often unfeasible due to experimental constraints such as equipment

and manpower, while simply counterbalancing across experiments is unsatisfactory because of the added variability. In this thesis, I use restricted randomization permutation testing to combine data across experiments and across sexes (for all experiments containing both males and females).

2.5 ANIMALS AND SURGICAL PROCEDURES

Animal housing

Environmental factors related to housing conditions, genetic variation and mouse handling are known to substantially affect behavioral in a wide variety of common laboratory tasks (Crabbe, et al., 1999; Bao et al., 1998). In an unpublished analysis, I noticed systematic variation in behavior even among distinct litters of animals of the same genotype. Thus, it is critically important to counterbalance all experimental groups across variables including littermates, sex, age, and housing conditions. Ideally, the all mice should be bred at the same time under similar conditions.

All behavior experiments were performed with mice housed on a reverse 12 h light/dark cycle (1000 h lights off) and provided with food and water *ad libitum*. Mice used in chapters 2 and 3 were housed in standard housing conditions, with 2-5 animals per cage and variable presence of paper hut and bedding square materials. In chapter 4, housing conditions were monitored more closely, with 2-4 animals per cage and consistent presence of paper hut and bedding materials for all group housed mice. For animals housed in social isolation, there was one mouse per cage and the paper hut and bedding square materials were removed.

Surgical procedures

Treatment of mice and surgical procedures were in accordance with National Institutes of Health guidelines and an institutionally approved animal welfare protocol. All mice were surgically implanted using a stereotaxic apparatus (Kopf) with custom-made stainless-steel head plates used for head fixation on a running wheel during training. Anesthesia was induced with 3% isoflurane mixed with oxygen and maintained with 2% isoflurane throughout the procedure. Animals were secured in a stereotaxic apparatus. Fur covering the head was removed with an electric shaver, then the skull was exposed by cutting away an 8-10 mm circle of skin such that both bregma and lambda were exposed. Fascia covering the skull was carefully removed, and the skull surface was gently etched with the tip of a scalpel blade. The cleaned and dried skull surface was covered in a thin layer of low-viscosity cyanoacrylate and the head plate was cemented on top with a layer of Metabond (Parkell). Rimadyl (5 mg/kg) was delivered subcutaneously at the neck and the mouse was transferred to a heated chamber to recover from anesthesia.

Some mice were additionally implanted with a tungsten stimulating electrode using a stereotaxic apparatus fitted with a custom-made electrode holder. This procedure resembled the head plate surgery with one additional step. After the skull was cleaned and etched, two 1 mm diameter craniotomies were drilled at AP 5.42 mm, ML +/- 2.25, At –2.25 mm (ipsilateral to trained eye), a tungsten electrode was lowered into the mossy fiber bundle 2.30 mm ventral to the brain surface. At +2.25 (contralateral to trained eye), a fully stripped ground electrode was lowered into the same AP coordinates, 1-1.5 mm below the brain surface. An extra layer of

Metabond was used to secure the electrodes. Mice were given a minimum of 4 days to recover before beginning acclimation to the running wheel and behavioral training.

1.9 CONDITIONING PROCEDURES

General conditioning

After recovering from surgery, animals began eyelid training. All training procedures took place in a dark behavior room during the animal's active cycle (1000 – 2200). Care was taken to ensure training procedures were carried out during similar times on each training day. On the first day, mice were acclimated to the experimenter by a two-minute handling session, where mice were placed in the gloved hand of the experimenter and allowed to explore. On the second day, mice were head-fixed to the training apparatus and acclimated for 15 minutes without delivery of any stimuli or camera recordings. On days 3-4, mice were further acclimated for approximately 30 minutes each day without stimulus delivery while 60, 1.2 s camera trials were collected to measure baseline levels of eyelid movement. Eyelid conditioning began on day 5 and lasted for 12-15 days, depending on the experiment. In some experiments, paired training was followed directly with two days of extinction and re-acquisition training, extending training to 24 days. For single-cue training, 60-75 trials were delivered each day. Chapter-specific methods provide more specific details on conditioning procedures.

Mossy fiber stimulation

For subjects trained with electrical stimulation of mossy fibers, the CS was a constant frequency pulse train of cathodal current pulses (50 Hz, 400 ms, 0.1 ms pulse width, 70 μA),

generated by a stimulus isolator (model A360, World Precision Instruments, Sarasota, FL) and passed through an epoxy-insulated tungsten electrode (A-M Systems Cat. 575300) implanted in the middle cerebellar peduncle ipsilateral to the trained eye (Kalmbach et al., 2010). Impedance at the tip of the electrode was adjusted to 100-200 kΩ). A fully stripped ground electrode was implanted contralateral to the trained eye at the same coordinates (see surgical methods, section 2.6). During behavioral sessions using mossy fiber stimulation, animals were head-fixed just as in peripheral cue training, then wire leads from the stimulus isolator were gently secured on the head stage leads. CS and US stimulus presentation were then delivered in the same configuration as peripheral cue training.

Acoustic startle response

In subjects tested for acoustic startle, a total of 20-30 pure startle tones (50 ms, 8 kHz, 85 dB) were presented during eyelid training sessions 2-5 in place of the CS-alone probe trial. Tones were generated as described in section 2.2.1. Since acoustic startle is a whole-body movement, startle can be detectable as a short latency (<10 ms) eyelid closure. Presence of startle was classified as an eyelid closure of above 0.05 fraction eyelid closure during the first 100 ms after tone presentation. Only startle probes that resulted in a startle response were used to assess startle magnitude.

1.10 HISTOLOGY

After behavioral training was complete, animals implanted with stimulating electrodes were further processed to map the site of electrical stimulation within the mossy fiber bundle.

Awake mice were head-fixed onto the running wheel used in behavioral training and a 30 μA constant cathodal current was passed through the electrodes for 15-20 seconds to mark the stimulation site. One to four hours later, mice were sacrificed with an overdose of ketamine/xylazine (0.25 ml of 10 mg/ml xylazine in 90 mg/ml ketamine) and perfused with PBS, followed by 4% formaldehyde/PBS. The entire head was removed, with head bar and stimulating electrodes intact. Perfused heads were then post-fixed for one week in formaldehyde/PBS. The heads were rinsed and stored in PBS overnight, after which the brains were removed from the skull. Brains were then rinsed and stored in PBS until sectioned at 50 μm on a VT1000S vibratome (Leica) and mounted on gelatin-coated glass coverslips.

Gelatin-coated glass coverslips were prepared by brushing glass Superfrost Plus glass slides (Fisher Scientific) with a 0.02% gelatin (product) dissolved in water. After slides dried for 36-48 hours, 50-micron brain slices were mounted and dried for at least 36-48 hours more. Finally, brain slices were stained with cresyl violet and imaged by light microscopy on an AXIOZoom V16 microscope (Zeiss).

Chapter 2: Enhanced eyelid conditioning in 3xTg model mice

2.1 INTRODUCTION

Alzheimer's Disease (AD) is a devastating neurodegenerative illness that remains poorly understood. AD refers to a complex form of neurodegeneration that destroys brain tissue with stereotypical anatomical progression, beginning with the entorhinal cortex, then spreading to the hippocampus, amygdala and neocortex. Histological examination of post-mortem tissue reveals characteristic extracellular protein aggregates called "plaques" and intracellular protein aggregates called "tangles".

The primary structures affected by AD are critical for memory and cognition, including the hippocampus, amygdala and prefrontal cortex. The first clinical symptoms include short-term memory loss and changes in emotionality and cognition. While cerebellar symptoms are observed in late stages of the disease or when specific Presenilin-1 mutations are involved (Lemere et al., 2006; Anheim et al., 2007), cerebellar pathology is typically not a prominent feature. Thus, the rationale for using eyelid conditioning to study learning in AD model mice is conceptually linked to the influence of the hippocampus, PFC and amygdala on cerebellar learning, as discussed in Chapter 1.

Preliminary studies (unpublished results by Dr. Jennifer Siegel) provided the surprising result that 3-4 month old 3xTg mice, an age reported to be free of severe pathology or memory deficits, exhibited more rapid eyelid conditioning compared to controls in the forebrain-dependent 'trace' eyelid conditioning task (50 ms CS, 250 ms trace interval). To verify and follow-up on this initial finding, I conducted a series of three experiments to gain insight into the

nature of this learning phenotype. Confirming and expanding on initial findings, I found enhanced eyelid conditioning in 3xTg animals in both trace conditioning and delay conditioning with a weak CS, two forms of the task that are known to require an intact forebrain. Differences in conditioning may be due to cue sensitivity due to heightened stress response, as I additionally found that 3xTg animals exhibit larger eye closures in response to acoustic startle, an independent measure of stress-sensitivity. The following section describes the experimental design and results of these three studies.

A note on Chapter 2 experimental design and statistical analyses

The experiments described in this chapter constitute a series of exploratory studies designed to gain information on eyelid conditioning in 3xTg mice. As a result, the experiments are largely under-powered, and many statistical comparisons fail to yield significant results. Further, similar experiments were combined in some cases, as described in detail in the subsequent sections. Thus, the results presented in Chapter 2 are intended to serve as a record and motivation for subsequent chapters rather than for statistical inference on a hypothesis. Descriptive statistics and statistical tests are performed to provide a complete description of the experiments but should not be interpreted as strict hypothesis tests.

The decision to abandon behavioral studies of 3xTg mice instead of repeating and expanding them was due to a lack of a proper wild-type control strain. We found that eyelid conditioning is highly sensitive to background strain of the animal (B6 vs 129S/B6 Hybrid vs 129S). Because 3xTg mice were created on a mixture background, it is not possible to have a proper control.

2.3 EXPERIMENT 1: TRACE VS. DELAY 300 MS ISI

Rationale and experimental design

This experiment aimed to confirm the initial findings that 3xTg mice outperform controls in trace conditioning (unpublished results by Dr. Jennifer Siegel), as well as to test the hypothesis that enhanced learning was specific to forebrain-dependent trace conditioning. Trace conditioning relies in part on persistent activity from the mPFC (a putative mechanism underlying working memory) while delay conditioning does not. Thus, learning differences between 3xTg and control animals should exist for trace conditioning but not delay conditioning.

A 2x2 design was implemented to test the effect of genotype (3xTg vs control) and the presence or absence of a stimulus-free trace interval (trace vs. delay) on conditioning in young (~4 months old) male mice. A "bright" light CS was used for training, functionally designated because forebrain-lesioned wild-type animals learn normally at this stimulus intensity in the delay task but not the trace task (Siegel et al., 2015).

In total, 44 Male 3xTg 129/B6 hybrid mice were conditioned in either trace (n=13 3xTg; n=12 129/B6 hybrid) or delay (n=12 3xTg, n=7 129/B6 hybrid). Mice were trained in either a trace (50 ms CS, 250 ms trace interval) or delay (300 ms CS) paradigm. Due to the large number of animals required, animals were trained in four cohorts. Three cohorts were fully counterbalanced across all experimental conditions, while the fourth consisted of only trace conditioning (4 3xTg and 4 129/B6 hybrid). Animals in cohorts 1-3 underwent 14 daily sessions of conditioning, while mice in cohort 4 received 11-14 sessions, with strong learners (> 80% CR) being retired early in this cohort.

To quantify learning, I chose two metrics to compare, learning onset and overall performance. For learning onset, I calculated the number of trials needed to reach a pre-defined behavioral criterion of 25% CR in a sliding window of 60 trials (Fig. 2.1C). For overall performance, I calculated percentage of CRs made during all behavior sessions for each animal. Because strong learners were retired as early as day 11, formal analysis of overall performance was restricted to behavior sessions 1-11.

Results

Trace conditioning is sensitive to mPFC lesions, while strong-CS delay conditioning is not. Poorer performance in trace conditioning is typical in wild-type animals and is thought to reflect increased task difficulty by requiring the PFC to supply a 'working memory' representation of the CS to the cerebellum during the otherwise stimulus-free trace interval. To identify learning phenotypes specific to trace conditioning in 3xTg animals, four groups were subject to eyelid conditioning: 3xTg-Delay, 3xTg-Trace, 129/B6 hybrid-Delay and 129/B6 hybrid-Trace.

Figure 2.1B shows group median learning curves with interquartile ranges for all sessions. Comparison of overall performance (Fig. 2.1C) showed significant differences among the groups (Kruskal-Wallis test, $p=0.046$). Follow-up pair-wise comparisons revealed a learning deficit specifically for trace-conditioned 129/B6 hybrid animals, while 3xTg-Delay, 3xTg-Trace, and 129/B6 hybrid-Delay mice produced a similar proportion of CRs.

3xTg-Delay, 3xTg-Trace, and 129/B6 hybrid-Delay mice also required a similar number of trials to reach behavioral criterion, while 129/B6 hybrid-Trace required an average of 454

trials (Fig. 2.1B-D). Although missing statistical significance (Kruskal-Wallis 4 group test, p=0.23), this is a notable trend.

The fact that 3xTg mice do not need additional trials to learn the trace task is notable and may be interpreted in (at least) two ways. First, it could mean that the CS-related signal generated by the PFC is stronger in 3xTg mice. Second, it could mean that the PFC signal arriving to the cerebellum is modulated by a third party, such as the amygdala. Since 3xTg mice have been shown to exhibit both deficits in forebrain-driven tasks (Stevens et al., 2015; Stover et al., 2015) and enhancement in amygdala-driven tasks (Stover et al., 2015) at this age, these results are may reflect amygdala driven modulation of CS-related inputs to the cerebellum.

Sensitivity to the unconditioned stimulus (US) can also modulate learning (Oswald et al., 2009). One measure of US sensitivity is the magnitude of the unconditioned response 'blink' made after presentation of the US. Four-group comparison of US magnitude during the first two training sessions just missed statistical significance (Kruskal-Wallis test, p=0.052). However, comparison of genotype (3xTg vs. 129/B6 hybrid) showed that 3xTg mice exhibited significantly smaller URs than 129/B6 hybrid (avg. magnitude of UR: 3xTg=24; 129/B6 hybrid=31, KS-test, p=0.019). Smaller UR magnitude in this particular experiment likely reflects downward adjustment of the US intensity to prevent the mouse from squinting rather than lower sensitivity to the US. That is, lower UR magnitude observed here likely reflects a lower threshold for 3xTg mice to develop chronic squinting to the US, meaning that US sensitivity is likely higher in 3xTg animals.

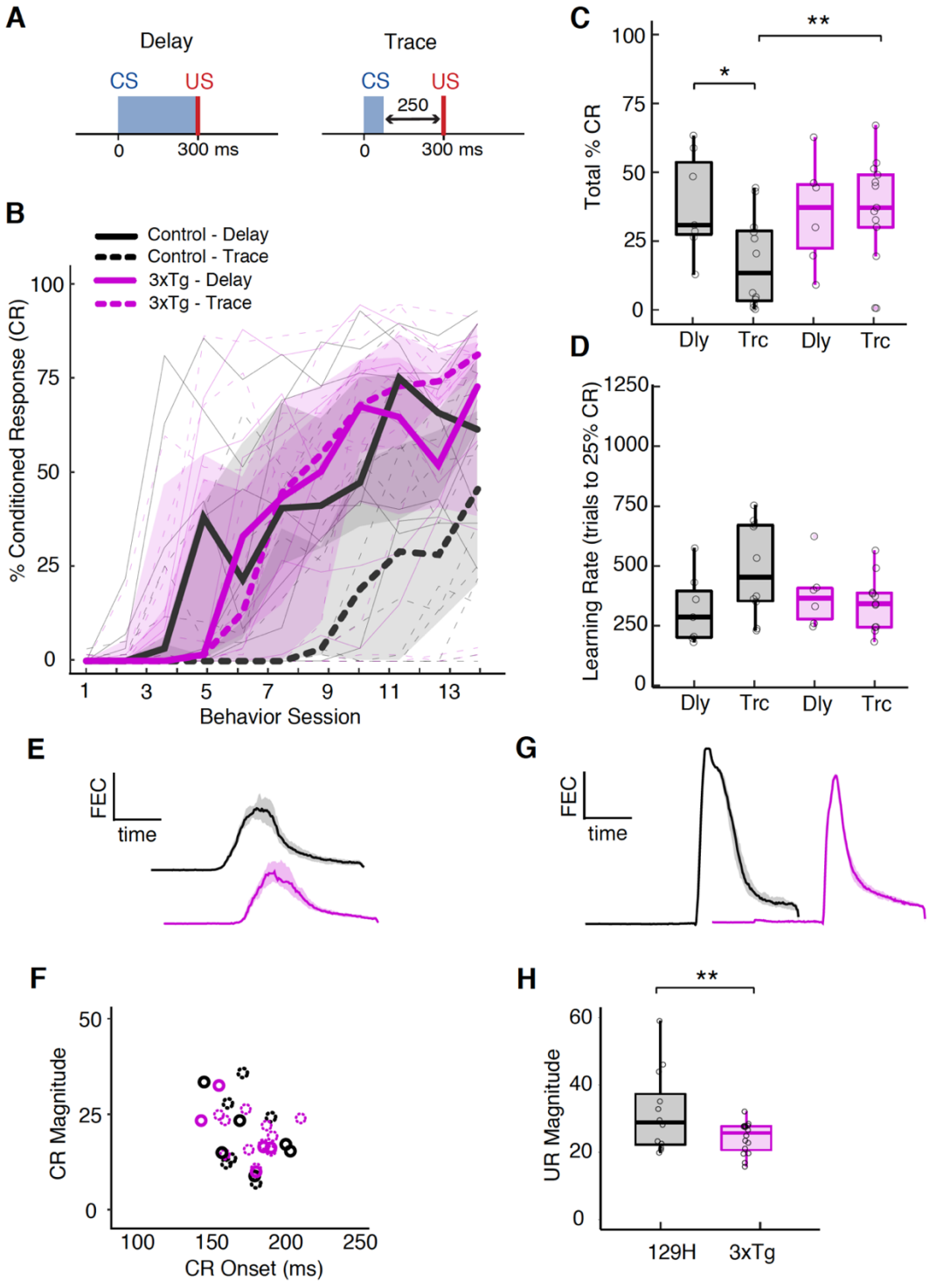

Figure 2.1: 3xTg animals do not show learning deficits in trace conditioning

Figure 2.1: 3xTg animals do not show learning deficits in trace conditioning

A. Stimulus figuration used in trace and delay conditioning. **B.** Group median learning curves shaded with IQR. **C.** Comparison of overall performance shows significant deficits in 129/B6 hybrid-Trace. (avg. overall %CR: 129/B6 hybrid-Trace=17%; 129-Delay=38%; 3xTg-Trace=36%; 3xTg-Delay=35%; Kruskal-Wallis test for 4 groups, p=0.047; followed by pairwise Conover Test without correction). **D.** Comparison of learning rate across the four groups reveals that 3xTg learn similarly with trace and delay conditioning, while control mice trend toward need more trials to learn the trace version of the task. **E.** Statistical summary of CRs from two representative animals. **F.** Two-dimensional clustering of CR properties shows that all groups produce similar motor responses. **H.** Interestingly, 3xTg animals displayed less reactivity to the air-puff US, likely a reflection of experimental manipulations to prevent animals from squinting.

2.4 EXPERIMENT 2: WEAK-CS DELAY CONDITIONING AND THE ACOUSTIC STARTLE RESPONSE

Rationale and experimental design

Results from Experiment 1 showed that 3xTg mice outperform non-transgenic controls in forebrain-dependent trace conditioning and show signs of US cue sensitivity raised the possibility that the behavioral phenotype is related to cue sensitivity in general, rather than specifically to a mPFC, 'working memory' phenotype. Cue sensitivity can be potentiated by an over-active amygdala. In light of this, I designed an experiment to simultaneously probe two different behaviors known to be modulated by the amygdala, weak-CS eyelid conditioning and the acoustic startle response (Weisz et al., 1992; Rosen et al., 1988).

Central amygdala projections to the caudal pontine reticular nucleus of the brainstem are necessary for stress-enhanced acoustic startle response in rodents. If enhanced conditioning in 3xTg mice is related to modulation of cerebellar inputs by amygdala projections to the basilar pontine nucleus in the brainstem, then other behaviors related to amygdala-brainstem modulation should also be altered in 3xTg model mice. The acoustic startle response (ASR) is one such behavior.

Briefly, the ASR describes the short latency (< 10 ms), full-body muscle contraction observed across mammalian species in response to a sudden loud noise. ASR relies on a tri-synaptic circuit from the cochlear nucleus in the ear, to the brainstem caudal pontine reticular nucleus, to skeletal muscles. Experiments in rats demonstrated that electrical stimulation of the central nucleus of the amygdala prior to a loud noise increases ASR amplitude (Rosen et al.,

1988), and pharmacological blockade of AMPA receptors in this region can prevent fear-potentiated ASR (Walker et al., 1997).

Animals and training procedure

Both male and female mice were used, aged ~6.5 months (3xTg, n=22 (5 female); n=22 129/B6 hybrid (9 female). Animals were combined across two experiments. Mice in the second experiment additionally received IP injections on training days 1-2, either kolliphor 4% vehicle or 30 mg/kg R121919. Null results of drug delivery in the second experiment, along with the exploratory nature of Chapter 2 permitted inclusion of both experiments. Genotypes were counter-balanced across both experiments.

Mice were conditioned in 12 daily conditioning sessions. Behavior sessions consisted of 60 paired CS-US trials and 5-7 startle probes. For startle probe trials, a 50 ms tone was presented instead of light and air-puff. Trials were presented in blocks of 5 as 4 consecutive paired followed by 1 startle probe. For more details, see section 1.9 (conditioning procedures). Startle data from only sessions 3-4 were used in the analysis. Startle data from sessions 1-2 were excluded because half of the animals in the experiment received IP injections on those days. Startle data from sessions 4-12 were excluded because those sessions included startle probes of lower intensity (75 dB) that did not elicit startle in most animals.

Results

To explore the possibility that enhanced learning observed in 3xTg animals is due to an amygdala-associated mechanism, I tested 3xTg mice in two behaviors known to be potentiated

by the amygdala under conditions of stress, eyelid conditioning and the acoustic startle response. Eyelid conditioning was tested using a weak-CS, delay 400 ms. Startle was tested in the same behavior sessions using a probe for acoustic startle (85 dB, 50 ms 8 kHz tone; See Fig. 2.4A). For weak-CS, LED brightness was adjusted to ~50% of bright CS used in Experiment 1.

3xTg mice perform only slightly better than controls in weak-CS delay conditioning

In contrast to trace conditioning, where 3xTg mice learn much better overall than controls, 3xTg animals do not show a higher CR rate overall nor do they learn in fewer trials (Fig. 2.2B,C,D). Comparison of learning rate (trials to reach 25% CR) revealed that 3xTg and controls reach behavioral criterion in a similar number of trials, avg. 3xTg=426; 129/B6 hybrid=439; Kruskal-Wallis test, stratified by sex, p=0.79. However, 3xTg mice may reach a higher plateau performance, as measured by percent CR during final two behavior sessions, as indicated by an insignificant trend toward higher plateau (avg. 3xTg=68%CR; 129/B6 hybrid=58%CR; Kruskal-Wallis test, stratified by sex, p = 0.08).

Next, I analyzed the prevalence and magnitude of the acoustic startle response (ASR). As a behavior known to be potentiated by amygdala-brainstem projections, ASR served as an independent measure of cue sensitivity potentially modulated by the amygdala. Prevalence of ASR, as measured by proportion of startle probes eliciting more than a 5% eyelid closure, showed that 3xTg mice made more startle responses than controls (Fig 2.3E; avg. 3xTg=66%; 129/B6 hybrid=49%; Kruskal-Wallis test, stratified by sex, p=0.045). Further, 3xTg animals produced ASR of larger magnitude (Fig 2.3F; avg. 3xTg=5.13; 129/B6 hybrid=1.60; Kruskal-Wallis test, stratified by sex, p=0.0096).

Overall, 3xTg mice displayed both slightly higher (not significant) performance in eyelid conditioning and a larger magnitude of the acoustic startle response. Because of the potentiated ASR, these results were consistent with an amygdala-driven cue-sensitivity phenotype in 3xT mice. Similar learning rates in weak-CS eyelid conditioning between the mutant and control animals could either mean that this form of conditioning does not differentiate the genotypes, i.e., the learning differences seen in trace conditioning are not due to cue sensitivity. Alternatively, the weak-CS intensity may not be optimal for this particular purpose.

One reason the CS cue may not be of optimal 'weak-CS' intensity is because the general equipment set-up and cue delivery system differed between Experiment 1 (trace vs. delay) and the current experiment (weak-CS delay). Although the 50% stimulus intensity compared to Experiment 1 was estimated by a light sensor (SparkFun ambient light sensor, TEMP6000), the 'weak' CS intensity used here may not be optimal for requiring forebrain engagement. A potential future experiment implementing a simple amygdala lesion could be used to identify an optimal light CS that requires forebrain input for learning.

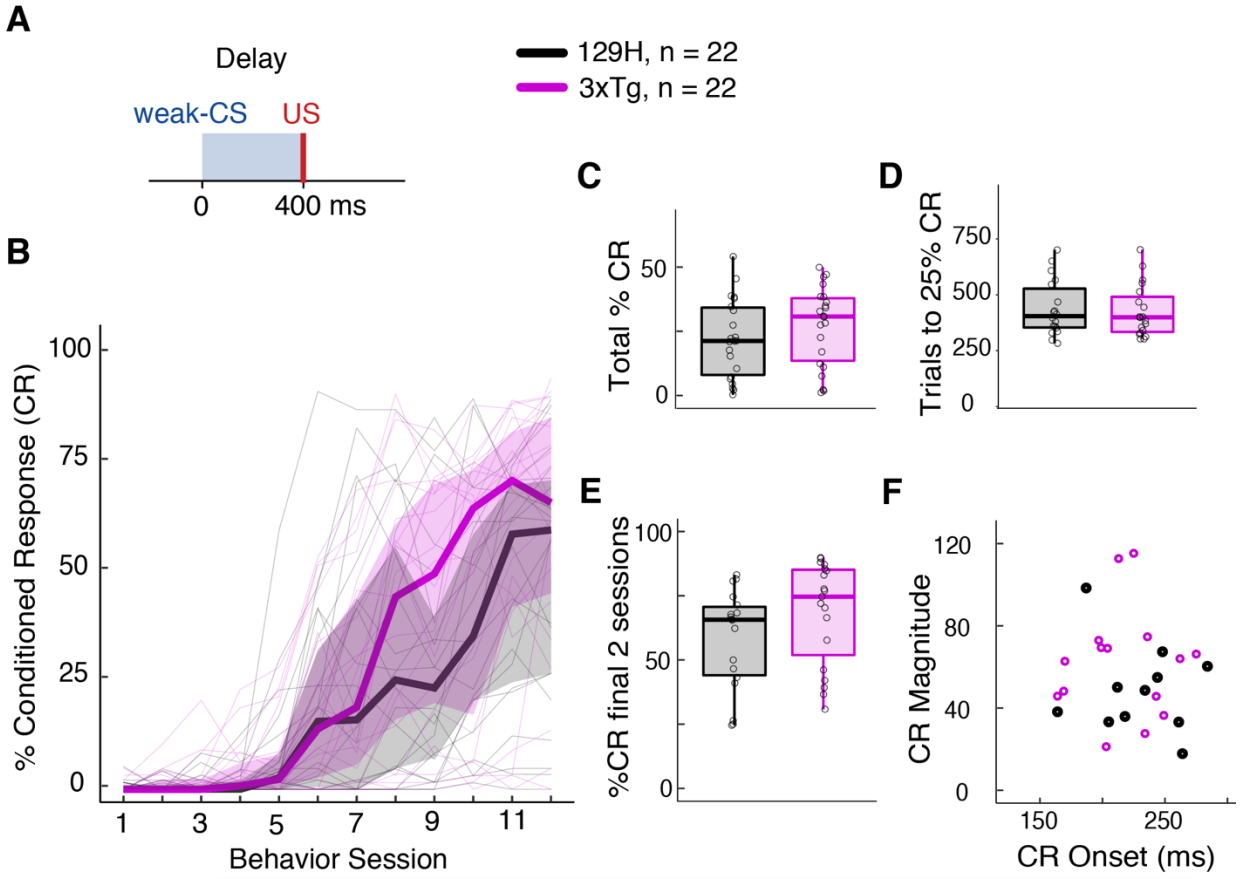

Figure 2.2: 3xTg mice achieve similar learning rate but higher performance in weak-CS delay conditioning.

A. Stimulus configuration used for weak-CS delay conditioning. **B.** Group median learning curves shaded with IQR. **C.** Overall performance does not differ significantly in 3xTg model (avg. 3xTg=27%; 129/B6 hybrid=22%, p=0.23). **D.** Both genotypes require similar number of trials to reach behavioral criterion (avg. 3xTg=426; 129/B6 hybrid=439; p=0.79). **E.** Comparison of plateau performance (final 2 behavior sessions) indicates that 3xTg mice may perform slightly better than 129/B6 hybrid in eyelid conditioning with weak-CS, although statistical significance was not achieved (avg. 3xTg=68%CR; 129/B6 hybrid=58%CR; p = 0.08), suggesting that 3xTg learning enhancement may not be restricted to trace conditioning. **F.** Two-dimensional clustering of response properties (onset and magnitude) show similar response properties in both genotypes. All comparisons were performed with Kruskal-Wallis test, stratified by sex.

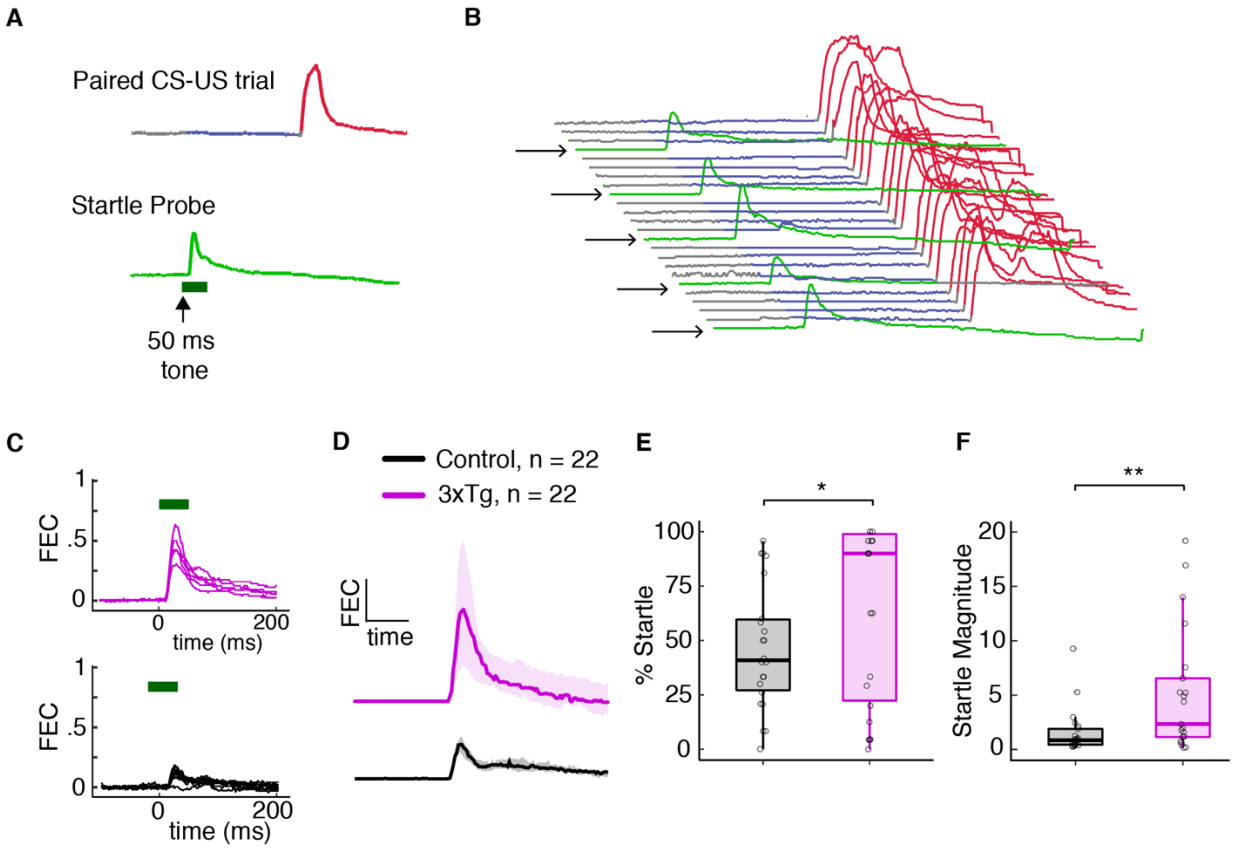

Figure 2.3: Larger acoustic startle in 3xTg mice.

A-B. Tone-only startle probes (green) delivered every 5th trial during weak-CS delay 400 ISI experiment (blue and red trace). Arrows indicate startle probes. **C.** Startle probes from one example 3xTg mouse (pink) and one example 129/B6 hybrid mouse. **D.** Group-median traces with bootstrap derived 95% CI illustrates larger startle probes overall in 3xTg mice. **E.** 3xTg mice generated more startle responses (avg. 3xTg=66%; 129/B6 hybrid=49%; p=0.045). **F.** 3xTg mice made larger magnitude ASR (avg. 3xTg=5.13; 129/B6 hybrid=1.60; p=0.0096). All comparisons were performed with Kruskal-Wallis test, stratified by sex.

2.6 EXPERIMENT 3: CONDITIONING IN AGED 3XTG MICE

Rationale and experimental design

AD is primarily a disease of aging. If enhanced associative learning observed in young 3xTg animals is related to forebrain hyperactivity that precedes neurodegeneration and cognitive decline, then aged 3xTg mice should have learning deficits in a difficult trace task that depends on an intact mPFC and other forebrain structures. However, if enhanced learning observed in young animals is instead due to an exaggerated stress response not related to cognitive decline, as implicated in Experiment 2, then aged mice may not display learning deficits.

To test this hypothesis, I probed learning in 3xTg and controls at ~16 months, an age when cognitive deficits have been measured in Morris water maze in 3xTg mice (Stevens et al., 2015). Thus, I hypothesized that aged 3xTg mice would show signs of cognitive decline, measured as learning deficits in eyelid conditioning. A one-way design was implemented to test the effect of genotype (3xTg vs 129/B6 hybrid) in a trace task in aged mice (50 ms CS, 350 ms trace interval). Aged-matched 3xTg (n=4) and 129/B6 hybrid (n=5) were trained for 12 daily sessions.

Results

Surprisingly, aged 3xTg mice did not show learning deficits as compared to controls. Figure 2.4B shows the learning curves for each genotype as well as the comparison of overall percentage of CRs. Aged 3xTg mice had higher CR rates, though not significant likely due to the small number of animals used in the study. At this age, 3xTg mice are known to display deficits

in spatial and working memory tasks such as Morris water maze (Sun X et al., 2005). However, 3xTg animals do not show deficits in a forebrain-dependent eyelid conditioning task, as shown here, even at an age when working memory deficits are readily apparent in other behaviors. Again, these results are most consistent with cue sensitivity phenotype, perhaps driven by the known stress-sensitivity phenotype of 3xTg animals.

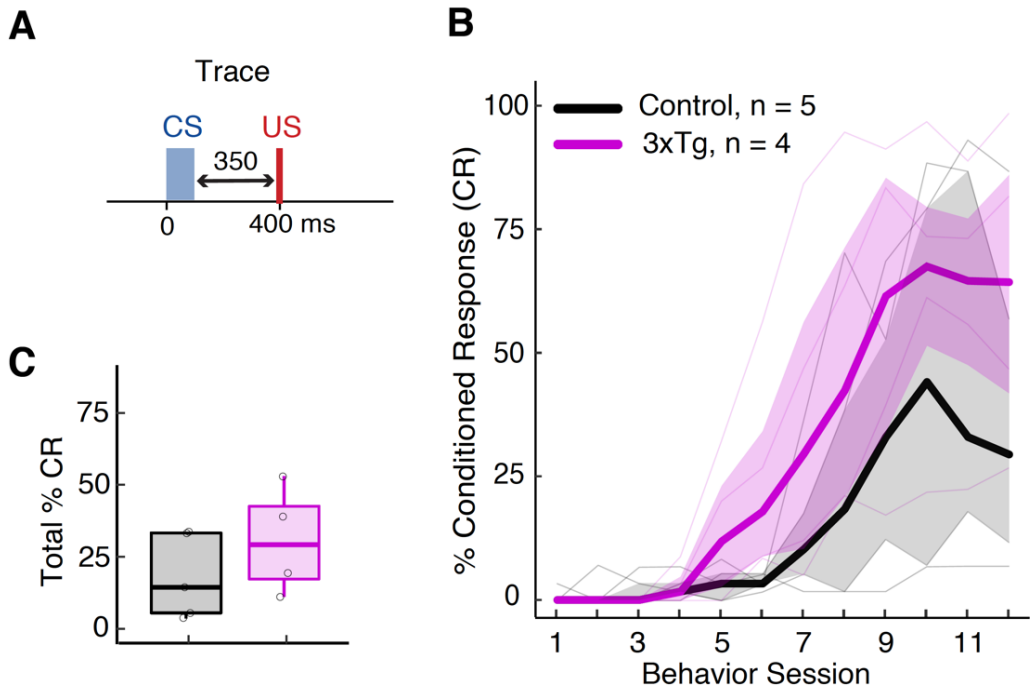

Figure 2.4: No learning deficits in 16-month-old 3xTg mice in forebrain-dependent task.

A. Stimulus figuration used for trace 50-350 conditioning. **B.** Group median learning curves shaded with IQR. **C.** Overall performance does not differ significantly in 3xTg model (avg. 3xTg=31%; 129/B6 hybrid=18%, p=0.56), even in aged animals when other forebrain-dependent tasks are impaired. All comparisons were performed with K-S tests.

2.7 DISCUSSION

Together, these results support a phenotype of cue-sensitivity in AD model mice, potentially driven by hyperactive amygdala-pontine modulation of cerebellar inputs. This result is notable because it provides behavioral evidence of enhanced associative learning in 3xTg mice and offers a platform on which to further disentangle and study the contribution of distinct, AD-relevant brain regions to learning.

Experiment 1 demonstrated that young 3xTg animals show similar levels of learning and behavioral performance during both trace and delay conditioning, while wild-type animals require more trials to learn in the trace task relative to the delay task, as previously reported in wild-type animals. One interpretation of this result is that forebrain hyperactivity in 3xTg mice, a known phenotype of APP/PS1 models (Busche et al, 2012) drives stronger persistent activity to the cerebellum, effectively eliminating the typical performance deficits observed during trace conditioning in wild-type mice (Fig. 2.1).

A second interpretation suggests that forebrain hyperactivity acts on cerebellar plasticity through amygdala-driven modulatory drive on inputs. More positive modulatory drive on sensory and persistent inputs could produce the same behavioral result. In this scenario, PFC-driven persistent activity is equal between the two genotypes and the observed behavioral advantage of the 3xTg model is instead due to stronger input arriving to the cerebellum due to pontine modulation. Experiment 2 revealed that enhanced conditioning in 3xTg mice is also observed under conditions of low CS intensity and thus is not exclusively linked to trace conditioning procedures.

PFC and amygdala influence on cerebellar learning are not mutually exclusive. It is possible that 3xTg mice may exhibit both altered persistent activity and heightened amygdala-driven modulation. However, these results provide important insights suggesting that amygdala modulation is a more plausible candidate mechanism. First, these results are not consistent with PFC dysfunction reported in AD models. Working memory deficits have been reported in several AD models, including 3xTg mice (Sun X et al., 2005). However, PFC lesions (Siegel et al, 2015) or manipulations that alter PFC excitability (Siegel et al., 2017) result in behavioral deficits in eyelid conditioning. If prefrontal contribution to eyelid conditioning relates to working memory, then deficit eyelid conditioning would be predicted, though it was not observed.

Second, enhanced associative conditioning observed in 3xTg animals was similar to those observed in rodent models of stress disorders. Rodent models of stress disorders display enhanced eyelid conditioning (both trace and delay) and higher levels of acoustic startle response than non-stressed mice (Shors et al., 1992, Weiss et al., 2005).

A critical link supporting this relationship between stress and AD models comes from the literature on Alzheimer's model animals. Anxiety and stress behaviors are common features of transgenic AD models. Indeed, APP/PS1 co-expression (such as the 3xTg model) results in higher corticosterone levels and stress behaviors than models expressing only mutant PS1.

A knock-in mutant APP mouse model demonstrates disproportionate sensitivity to restraint stress compared to non-transgenic controls, resulting in elevated corticosterone levels, increased acoustic startle, and fewer light entries in a light-dark box test (Justice et al., 2015). This study additionally established that amyloid-β peptide can directly activate corticotropin-releasing factor type-1 receptor, a known mediator of the stress response. In turn, glucocorticoids

released as part of the stress response feedback to exacerbate amyloid-β pathology in 3xTg mice (Green et al., 2006).

The 3xTg model in particular displays stress sensitivity, including more anxiety-related behaviors in open-field and elevated plus maze, and higher levels of freezing in fear conditioning. Mild social stress from pairing unfamiliar male mice caused a disproportionate increase in corticosterone, exacerbated amyloid-β pathology, and increased stress behaviors in 3xTg animals compared to wild-type or 3xTg mice not exposed to novel males (Rothman et al., 2012).

A separate Alzheimer Disease model, based on APPswe and PS1dE9 (a different PS1 mutation causing familial AD) also exhibit more amyloid-β pathology and elevated corticosterone after daily exposure to a novel environment, as compared to wild-type or mutants not exposed to novel environment (Stuart et al., 2017). Social isolation is another form of stress reported to have a disproportionate effect in the Tg2576 model overexpressing an APP mutation. After 6 months of social isolation, mutant mice display elevated corticosterone and increased plaque formation (Dong et al., 2008).

That APP models are often reported to show higher levels of stress and anxiety is an interesting point. While APP-based mouse models are reported to display more severe anxiety and stress-sensitive behavioral phenotypes than the knock-in PS1 model (Guo et al, 2012; Justice et al., 2015), PS1 mutations lead to more severe AD progression and earlier age of onset than do APP mutations in the human population (Ryman et al., 2014). Although this is observational evidence, it lends support to the idea that amyloid-β exacerbation of anxiety phenotypes observed in rodent AD models may be related to a biochemical process that is separate from the

primary cause of AD. Although this separate mechanism can exacerbate AD pathology (Guo et al, 2012; Justice et al., 2015), it is possible that this is a separate feature of AD mutations not directly responsible for cognitive decline.

Chapter 3: Interaction of stress and mutant copy number on eyelid conditioning in PS1 mice

3.1 INTRODUCTION

Mouse models of Alzheimer's disease (AD) were historically designed with the goal of over-producing neurotoxic amyloid-β, a characteristic peptide found in post-mortem tissue of AD patients. However, failure of clinical trials designed to remove amyloid-β from patients suffering from the disease have demonstrated that the peptide likely does not have a simple causal relationship with AD (Mullane et al, 2018). Mice that produce high levels of the peptide, far above the amount observed in human tissue, have been reported to display behavioral phenotypes indicative of an over-active stress response. This curious property of many AD models is not reflected in the human population and suggests that excess amyloid-β may be related to stress sensitivity independent of its role in the neurodegeneration and cognitive dysfunction central to the devastating manifestation of the human disease.

In this chapter, I examine learning in the PS1M146V knock-in model which only mildly over-produces amyloid-β. The vast majority of familial inherited Alzheimer's disease mutations, including the most severe as measured by age of symptom onset, are found in the *PS1* gene (Ryman et al., 2014). PS1M146V knock-in mice aged 3 or 9 months displayed spatial and working memory deficits, as measured by the Morris water maze test (Sun X et al., 2005), and deficits in contextual fear conditioning at 3 months of age (Wang et al., 2004). Thus, although the knock-in PS1 model does not produce the high levels of amyloid-β seen in the other models, it does capture spatial learning and memory deficits relevant to human AD.

To investigate learning in a more biologically realistic model of AD, I probed eyelid conditioning in single- and double- PS1M146V mutants, and their littermates expressing two wild-type copies of PS1. In sharp contrast to aged 3xTg animals, which exhibit rapid learning likely due to cue sensitivity, aged single mutants exhibit learning deficits as compared to their wild-type littermates. Double mutants display an intermediate rate of CRs, suggesting that two mutant copies may rescue the learning deficit observed with one mutant copy.

Since environmental stress is known to exacerbate AD pathology and the stress response, I also tested the effect of social isolation stress on both single-and double- mutants as compared to their wild-type littermates. In the case that mutant PS1 confers stress sensitivity not readily apparent under basal conditions, I predicted that a more severe stress phenotype would be seen in PS1 double mutants compared to single-mutants or wild-type littermates exposed to the stressor.

3.2 METHODS

Animals

Male and female mice were used in all experiments. Mice were generated by crossing PS1 heterozygous (PS1/WT) mice stabilized to 129/B6 hybrid background strain for six generations. The *PS1* knock-in used in the study was generated by knocking in only a short sequence with the *PS1* gene containing the M146V mutation and a humanized sequence around the mutation. This strategy left the rest of the gene as the mouse sequence, further reducing the chance for off-target consequences (Guo et al., 1999). Thus, offspring of these mice included

humanized *PS1* double mutants (PS1/PS1), humanized *PS1* single mutants (PS1/WT) and littermate wild-types (WT/WT) that had two copies of mouse wild-type PS1.

After recovering from surgery, mice were acclimated to the behavioral rig and head-fixation for 4 days prior to behavioral training. Animals underwent 15 days of paired training, with each day consisting of 75 trials (60 paired and 15 probe). Due to age-related vision impairments common to aged mice, CS intensity was doubled as compared to the weak-CS delay experiments.

To induce stress by social isolation, a subset of the mice from each genotype were separated from their littermates and housed alone for 4 months prior to the start of the experiment. Aside from housing conditions, socially isolated mice were bred and treated exactly the same as their littermates that were group housed.

3.2 RESULTS

Learning deficits revealed in group-housed single but not double mutants

In order to evaluate overall learning across genotypes, I calculated the total percentage of conditioned responses made by each animal across all 15 behavior sessions (Fig. 3.1C, avg. WT/WT=19%; PS1/WT=9%; PS1/PS1=13%, Kruskal-Wallis 3-group test, $p = 0.047$. Pairwise Conover test for WT/WT vs. PS1/WT, $p=0.0087$). Group median learning curves for each genotype showed that wild-type mice learned the task better than single-mutants, with double mutants showing intermediate levels of learning (Fig. 3.1B). The learning differences between the groups were driven by the high level of non-learners in the single-mutant group (6/12) as

compared to non-learners in wild-type (2/12) or double mutant mice (0/13). Among the learners, there were no differences in how many to reach the behavioral criterion of 25% CR (Fig. 3.1D, avg. WT/WT=774; PS1/WT=820; PS1/PS1=835, Kruskal-Wallis 3-group test, $p = 0.58$).

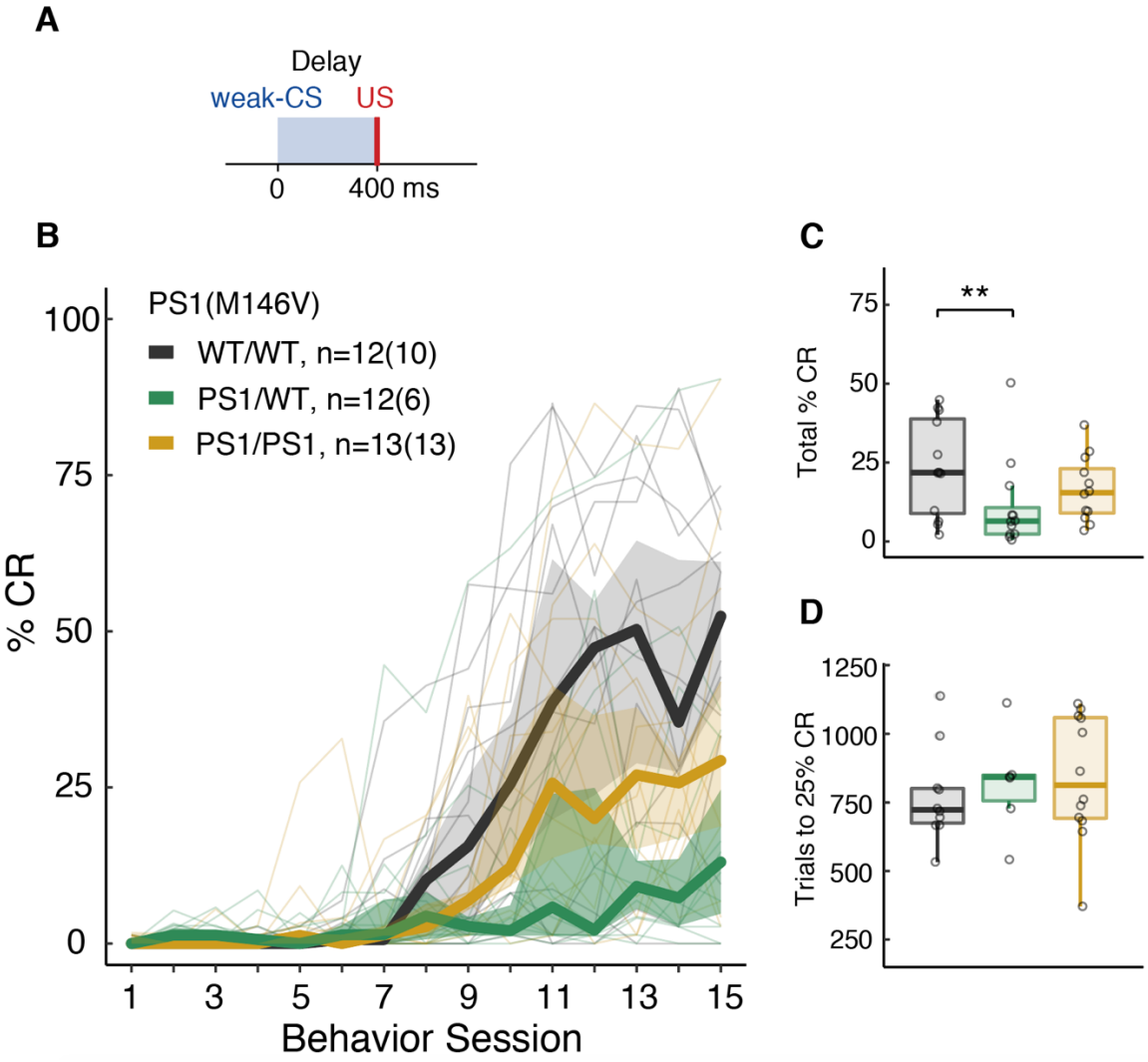

Figure 3.1: Single mutants exhibit learning deficits in weak-CS delay conditioning.

A. Stimulus configuration for delay 400 ms ISI conditioning. **B.** Learning curve over 15 days of paired training for littermate mice harboring either one copy of mutant PS1M146V (green), two copies (green) or two wild-type copies (black). Thin lines represent individual animal data, while thick lines represent group medians surrounded by shaded interquartile range of each group. Data for all animals is plotted in **B**, with the number of subjects per group indicated. The adjacent number in parentheses gives the number of mice classified as "learners", achieving 25% CR over all training in a sliding window of 60 trials. **C.** Single mutant mice show fewer CRs overall (three-group Kruskal-Wallis test, stratified by sex, p=0.047, followed by pairwise Conover Test without correction. See text for results.). **D.** It took all groups similar number of trails to reach learning criterion (Kruskal-Wallis test, stratified by sex, p=0.58). Notice that low performance in single mutant mice was driven by a high proportion of non-learners.

Learned motor responses are similar across genotypes

To compare motor response properties, only animals that made at least 80 CRs and reached at least 25% CR sometime during training were analyzed. Therefore, non-learners were not included in analysis of conditioned response properties. To control for learning, only responses 21-80 were compared for each animal. Analysis of conditioned response properties revealed similar responses across the three groups (Fig. 3.2), indicating that the learned motor response did not differ among the genotypes.

Double mutants produce larger unconditioned responses

Analysis of unconditioned responses to the air-puff stimulus during the first two behavior sessions revealed a group effect on UR magnitude (Fig. 3.3D, avg. UR magnitude WT/WT=46; PS1/WT=40; PS1/PS1=57, Kruskal-Wallis 3-group test, $p = 0.033$). Follow-up pairwise comparison indicated that PS1 double mutants made larger URs than either wild-type or single mutants, a phenotype that may indicate stress sensitivity. Interestingly, these findings indicated that double mutants have larger URs than wild-type, but still perform more poorly. This supports the notion that the modest recovery in learning seen in the double compared to the single mutant may be due to a distinct influence on learning arising from a heightened stress response in these animals.

To understand how learning outcomes are related to UR magnitude within genotype, I compared UR magnitudes within genotypes depending on learning outcomes ("learners" vs. "non-learners"). Due to small numbers of non-learner in wild-type and double mutant groups, it was not possible to test if UR magnitude predicted learning in these groups. However, URs made

by the 6 double mutant non-leaners had a median value ~50% lower than that of the 6 single-mutant learners (Fig. 3.3J). Thus, it is possible that learning deficits in single-mutant animals are driven at least in part by lower sensitivity to the US and this should be tested in future experiments designed to measure this aspect of the behavior.

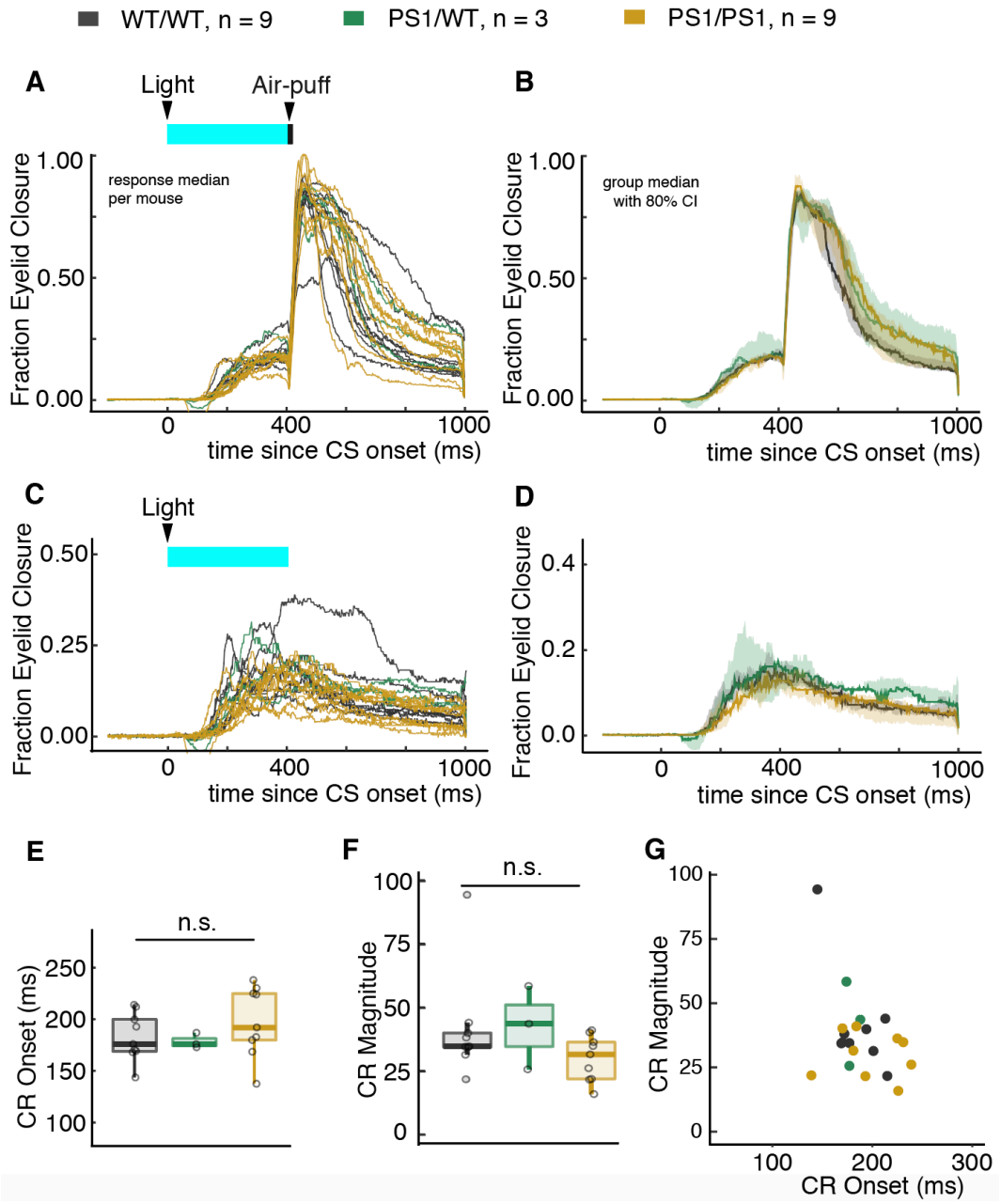

Figure 3.2: Similar CR properties in PS1 mutants and their wild-type littermates.

Single and double mutants display conditioned response properties similar to wild-type littermates. Single animal response medians are overlaid for paired (**A**) and probe (**C**) trials from the first 21-80 CRs made per animal. **B** and **D** depict the group-median and 95% confidence interval of the single animal summaries in **A** and **C**. **E-F**. Kruskal Wallis tests, stratified by sex, were performed on median CR Onset ($p = 0.49$) and CR magnitude ($p = 0.58$). **G**. Two-dimensional clustering further supported similar response properties across genotypes.

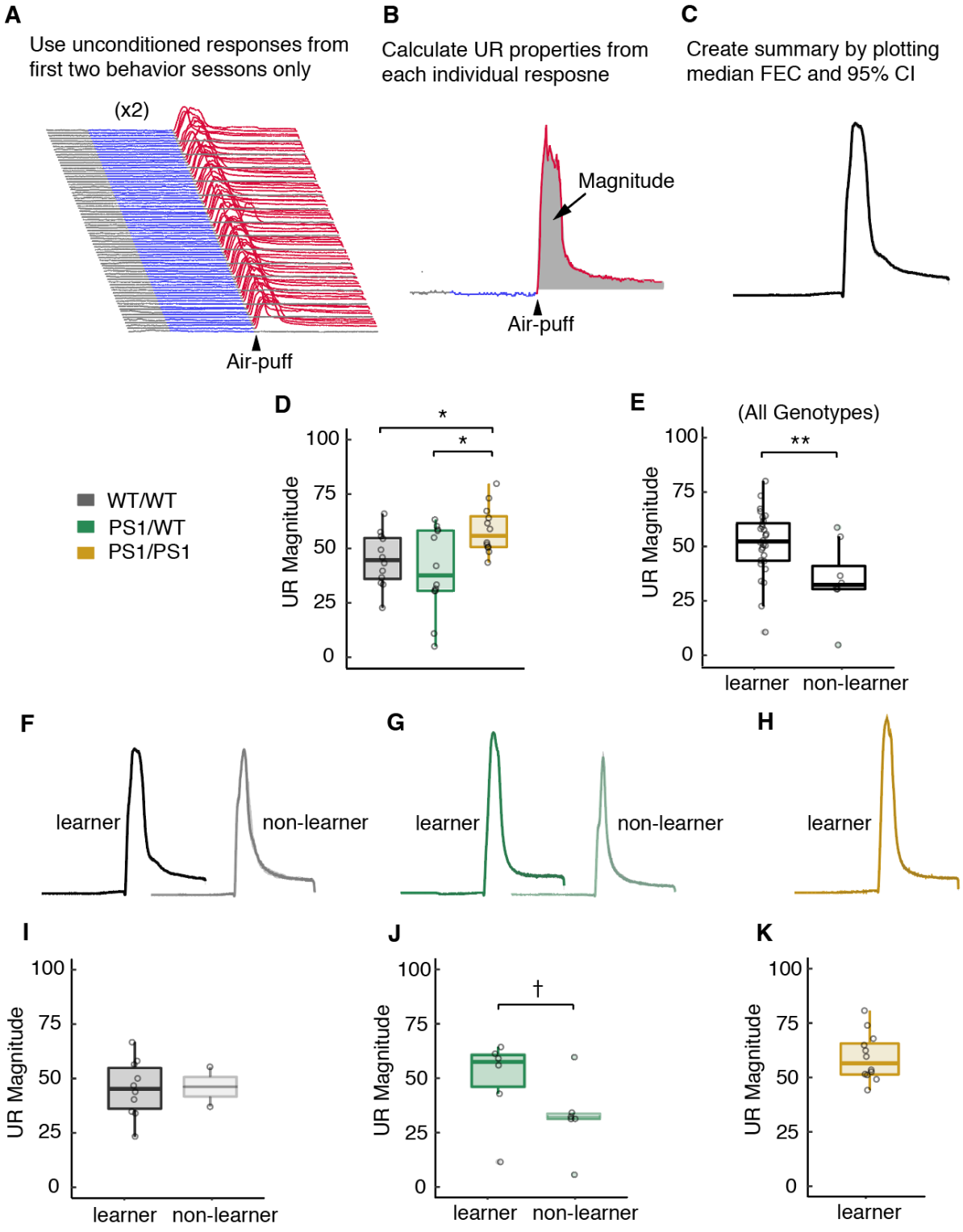

Figure 3.3: Double mutants are more reactive to the unconditioned stimulus

Figure 3.3: Double mutants are more reactive to the unconditioned stimulus

A-C. Derivation of UR measurements. URs from first two behavior sessions were measured to avoid contamination from the CR. **D.** double mutants showed larger URs than single mutant or wild-type mice (Kruskal-Wallis 3 group test stratified by sex, p=0.33, followed by uncorrected Conover-Iman pairwise comparison: PS1/PS1 vs PS1/WT p =.0014; PS1/PS1 vs. WT/WT p=0.018). **E.** Across genotypes, animals that did not reach behavioral criterion displayed significantly lower magnitude URs. **F-H.** Statistical summary traces from a 'learner' and 'non-learner' from each genotype, along with **I-J.** group-wise comparison of median UR magnitude per animal. Although sub-groups are too small for reliable comparisons, the smaller magnitude of single mutant non-learners is noteworthy.

Learning and response properties in socially isolated mutants

Next, I asked how social isolation stress influences eyelid conditioning in single- and double mutant mice. Social isolation has been found to interact with mutant APP overexpression, disproportionately increasing corticosterone levels and amyloid-B load in mutant mice after 6 months of isolation as compared to non-stressed transgenic or stressed controls (Dong et al., 2008). However, it is unclear if the same interaction occurs with PS1 mutants, and if it is related to the number of mutant copies (PS1/PS1 vs. PS1/WT).

In order to evaluate learning across the three genotypes, mice were isolated for 4 months leading up to the experiment, and then were trained in a delay 400 ms eyelid conditioning task. A large proportion of the single and double mutant isolated mice died before four months of isolation, yielding under-powered comparisons. Nonetheless, I calculated the learning curves and total percentage of conditioned responses made by each animal across all 15 behavior sessions (Fig. 3.4C). Comparing overall percentage of CRs revealed that wild-type and single mutants produced a similar amount of CRs, while double mutants showed a non-significant trend toward greater overall CR proportion. Learning rate comparisons showed that wild-type and single mutants needed a similar number of trials to reach behavioral criterion, while double mutants showed a notable trend toward faster learning than either wild-type or single mutants (Fig. 3.1C). Similar levels of non-learners were observed among the genotypes. Careful analysis of conditioned response properties revealed no differences in CR properties across the genotypes (Fig. 3.5).

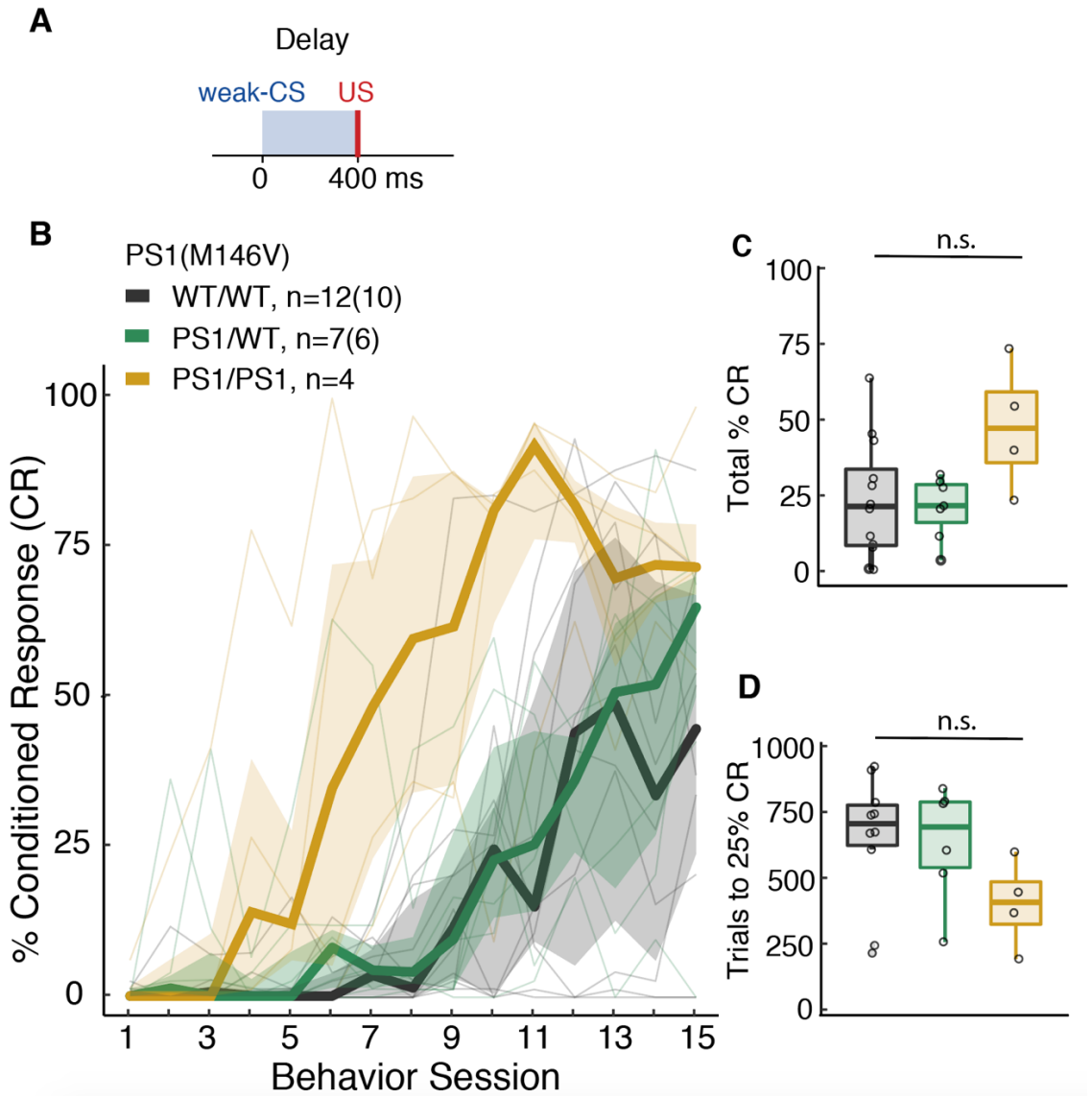

Figure 3.4: Similar learning properties in socially isolated mutants.

A. Stimulus configuration for delay 400 ms ISI conditioning. **B.** Learning curve over 15 days of paired training for mice following four months of social isolation, harboring either one copy of mutant PS1M146V (green), two copies (green) or two wild-type copies (black). Thin lines represent individual animal data, while thick lines represent group medians surrounded by shaded interquartile range of each group. Learning curves for all animals are plotted in **B**, with indicated number of subjects per group. The adjacent number in parentheses gives the number of "learners" per group, classified by achieving 25% CR over all training in a sliding window of 60 trials. **C.** Total %CR shows no significant overall group difference in total CRs produced ($p=0.11$), and **D.** learning rate also does not significantly differ in among stressed mice ($p=0.12$). Significance determined by Kruskal-Wallis three-group test, stratified by sex.

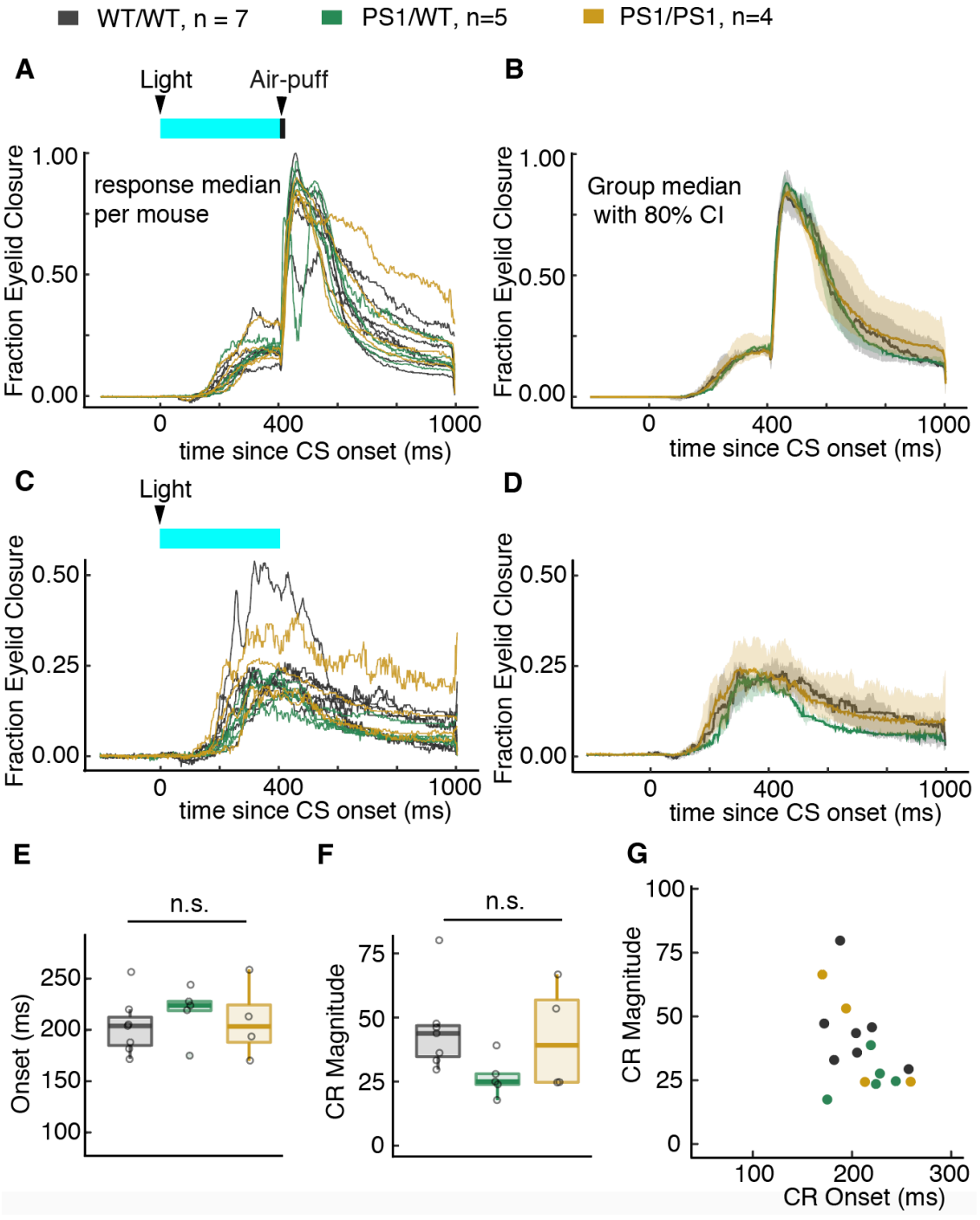

Figure 3.5: CR properties unchanged in stressed single and double PS1 mutants

Figure 3.5: CR properties unchanged in stressed single and double PS1 mutants

Single and double mutants display conditioned response properties similar to wild-type littermates. Single animal response medians are overlaid for paired (**A**) and probe (**C**) trials from the first 21-80 CRs made per animal. **B** and **D** depict the group-median and 95% confidence interval of the single animal summaries in **A** and **C**. **E-F**. Kruskal Wallis tests were performed on median CR Onset ($p = 0.70$) and CR magnitude ($p = 0.088$). **G**. Two-dimensional clustering further supports similar response properties across genotypes.

Stress preferentially enhances learning in mutant mice

In the previous experiment examining learning properties in socially isolated mutant and wild-type animals, many of the single and double mutant mice died before the start of the experiment. Therefore, group numbers for both single and double mutants were lower than planned, and statistical analysis of learning properties failed to reveal any group differences. Keeping in mind the under-powered nature of the social-isolation experiment, there is an obvious trend toward rapid learning in double mutants (Fig. 3.4). Additionally, notice that socially isolated single mutants do not show learning deficits compared to wild-type mice as they do in the absence of isolation stress.

In light of the different levels of learning observed among the genotypes in group-housed mice, a more informative analysis of the effect of stress on learning was to compare the effect of stress within each genotype to understand how stress interacts with mutant PS1. Social isolation stress induces significant enhancement of learning uniquely in single and double mutant animals (Kruskal-Wallis tests, $p=0.022$ and $p=0.0050$, respectively) while social-isolation does not induce enhanced learning in aged wild-type animals ($p=0.68$). Although social isolation is a potent stressor in young wild-type mice, the four-months of social isolation stress implemented in this study may be mild for wild-type aged-mice, who seems to be less sensitive to the effects of social isolation than their juvenile counterparts.

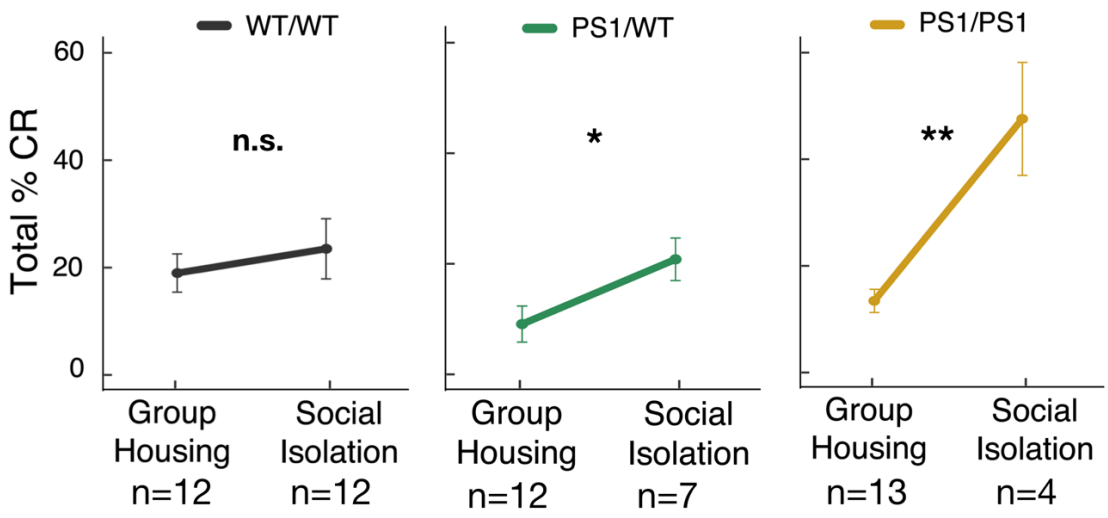

Figure 3.6: Stress preferentially enhances learning in mutant mice.

Overall learning measured as total %CR for group-housed and socially isolated wild-type (black), single (green) and double mutant (yellow) mice. Four-months of social isolation did not significantly affect learning in wild-type mice (avg. total %CR: group-housed=19%; social isolation=23%, p=0.68). However, social isolation induced enhanced learning single-mutants (avg. total %CR: group-housed=9%; social isolation=21%, p=0.022) and in double mutants (avg. total %CR: group-housed=13%; social isolation=48%, p=0.0050). Plotted values are mean with standard deviation in each case. Significance assessed with Kruskal-Wallis tests, stratified by sex.

3.3 Discussion

This study is the first to examine the interaction of mutant PS1 copy number with chronic stress in an associative learning task. The data indicate the existence of two dissociable behavioral phenotypes associated with PS1 mutations. The first relates to learning deficits, as seen in the single mutant, non-stressed mice. The second phenotype is related to enhanced associative learning and is associated with the interaction between stress and PS1 mutations.

Single-copy inheritance is how the gene is passed on in the human population. Interestingly, this is the only mode of inheritance (among 3xTg, PS1/WT, PS1/PS1) that resulted in learning deficits in a forebrain-dependent task. Importantly, the learning deficits observed in this group are most consistent with memory deficits in the human population. Although more research is needed to understand the behavioral and biochemical consequences of expressing multiple mutations, these results indicate that a qualitatively different outcome can result in aged AD model animals, dependent on mutant copy number.

The enhanced associative learning phenotype was observed to be a function of mutant copy number and stress. In un-stressed mice, a second copy of mutant PS1 rescues the learning deficits from having only one mutant copy. In stressed mice, learning is rescued in single mutants as compared to their unstressed counterparts. Finally, double mutants exhibited the most dramatic enhancement of learning after social isolation stress.

Interaction of stress and AD-causing mutations in mouse models

Although biochemical data is needed to identify an underlying mechanism of the present findings, one explanation for this behavioral dissociation is driven by the stress response and over-production of amyloid-β peptide (Fig. 3.6). Several studies have reported a stress-gene interaction in mutant APP and mutant APP/PS1 mice that results in increased amyloid-B production (Dong et al., 2008; Justice et al., 2015; Stuart et al., 2017). In one particularly comprehensive study (Justice et al., 2015), a mutant APP knock-in line demonstrated this stress-gene interaction.

In addition to demonstrating increased amyloid-β and anxiety behaviors after stress in APP mutants, the researchers were able to make a connection to a possible mechanism. Amyloid-β peptide can directly activate corticotropin-releasing factor type-1 receptor, and genetic deletion of the receptor can prevent the stress-gene interaction.

In contrast to mutant APP based models, there is a lack of research into the interaction of environmental stress with PS1 mutations. One study conducted in a mutant PS1 transgenic (overexpressing) line found stress-gene interaction in hippocampal neurogenesis. Unstressed transgenic mice overexpressing mutant PS1 were found to have lower numbers of newborn cells in the dentate gyrus as compared to unstressed controls. However, after a chronic intermittent restraint stress protocol, mutant PS1 mice showed higher levels of doublecortin as compared to non-stressed mutant PS1 mice (Kunimoto et al., 2010).

Stress as a risk factor for AD in the human population

The relationship between stress and AD in humans is well-documented. Incidence of PTSD in a large cohort of veterans was found to increase the incidence of AD two-fold (Yaffee et al., 2010). Additionally, self-reported general anxiety appears to be associated with an increased incidence of AD (Petkus et al., 2016). In addition to psychological stress, physical stress in the form of traumatic brain injury increases the incidence of AD. Both traumatic brain injury and PTSD have been shown to increase amyloid-β using PET scans in humans (Johnson et al., 2012; Mohamed et al., 2018).

However, it is important to note that neither physical nor psychological stress causes AD with 100% penetrance, as is the case with inherited mutations in APP or the Presenilin-1. Most

people with stress disorders will likely not go on to develop AD, and those experiencing traumatic brain injuries are also not guaranteed diagnosis. Biochemically, this is mirrored by amyloid-β load: not all people with high levels of amyloid-β develop AD, and not all people who develop AD have a high amyloid-β load.

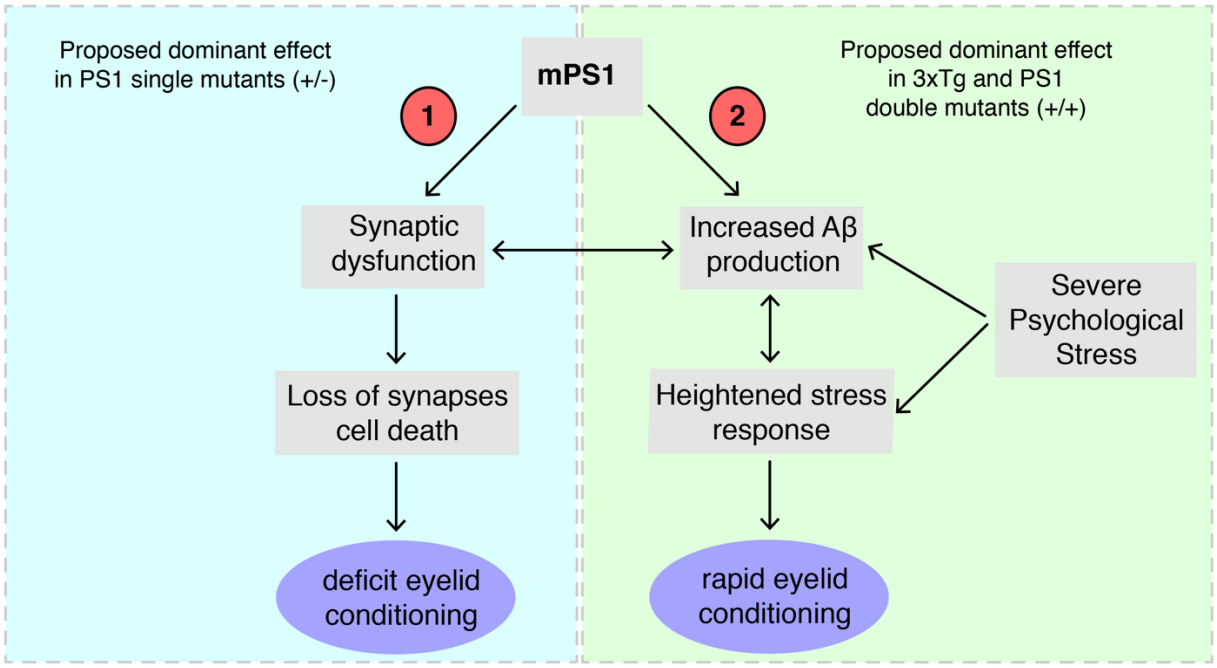

Figure 3.7. Interpretation of PS1 behavior and proposed model to be tested

Results from stressed- and un-stressed PS1 behavior experiments, as well as literature review of other behaviors in AD models, support a two-mechanism model of mutant PS1 (mPS1) dysfunction. The first mechanism (the one that is likely to be directly responsible for cognitive decline), involves PS1 contribution to synaptic functioning and is not linked to amyloid-β production. This pathway may be the cause of the learning deficit observed in aged single mutants and is consistent with cognitive decline associated with familial AD disease inheritance in the human population, which occurs as single-copy inheritance. The second mechanism relates to the overproduction of amyloid-β peptide, a common feature of mouse models of AD and a metabolite that is linked to the brain's stress response. Since PS1 double mutants and 3xTg animals produce more amyloid-β peptide, this may explain why their behavioral phenotype is dominated by stress sensitivity, measured in this study as rapid eyelid conditioning. This mechanism could also explain why psychological stress (in these experiments, social isolation) also leads to enhanced eyelid conditioning.

Chapter 4: Distinct effects of acute and chronic stress on eyelid conditioning

4.1 Introduction

Severe acute or chronic trauma can result in pathological remodeling of neural circuits that profoundly affects memory and cognitive function, the proposed biological substrate of stress disorders such as generalized anxiety disorder and post-traumatic stress disorder (PTSD). Two rodent models of PTSD are based on either acute trauma (Rajbhandari et al., 2018) or social isolation (Pibiri et al, 2008). Both models reproduce key features of PTSD, including enhanced associative learning. These features are accompanied by alterations in neural circuits important for cue processing and emotionality, such as the PFC, hippocampus and amygdala.

However, there are important differences in these two forms of stress that suggest different pathophysiological effects on the brain. For example, these two forms act on very different timescales. Traumatic stress, such as that experienced as a result of car accident or by an act of violence, acts on a relatively short timescale, sometimes exerting long-lasting changes in neural circuitry after just one exposure. On the other hand, social isolation and other chronic stressors can take weeks or months to cause lasting changes in the brain.

In this chapter, I employed eyelid conditioning as a behavioral assay to compare learning in two forms of PTSD: chronic social isolation and acute electric shock. Both forms of stress resulted in higher overall rates of CRs than in unstressed littermate controls. This result was similar in both males and females and is consistent with other reports of enhanced eyelid conditioning after stress. Interestingly, response timing analysis revealed a shortened latency to response onset uniquely in shock-stressed mice, but not in isolation-stressed mice. This

discrepancy between shock-stress and isolation stress may reflect distinct mechanisms by which shock and isolation affect the brain. Alternatively, it may reflect the longer timescale of isolation stress. That is, the lack of shortened response latency in isolation mice may be due to the prolonged nature of the stress exposure, allowing time for compensatory mechanisms to act and correct response timing.

Next, I used direct electrical stimulation of the mossy fiber bundle to test the hypothesis that enhanced learning after social isolation stress is specifically due to stronger inputs arriving to the cerebellum by the mossy fiber pathway. By using a mossy fiber stimulation as a CS, I was effectively able to control CS-related inputs to the cerebellum. Indeed, stress-induced learning differences disappeared when intensity-controlled mossy fiber stimulation was used as CS, revealing that differences in mossy fiber inputs to the cerebellum can fully account for learning differences in stressed animals. Interestingly, response timing analysis of animals trained with mossy fiber stimulation revealed a combination of longer latency responses and smaller magnitude responses. This finding suggests that the cerebellum may adapt to the stress-induced long-term changes in input strength by reducing learned output and may help explain why short-term acute stress drives shorter latency responses while chronic stress does not.

4.2 Effects of social isolation stress on eyelid conditioning

Methods

Male (n=16) and female (n=12) 129S1/SvImJ (129S) mice were used. To induce social isolation stress, 14 mice were removed from standard group housing at ~3 months of age. Mice remained either with cage-mates (control; n=14, 6 female) or in social isolation (stress; n=14, 6 female) for

8 weeks prior to the start of conditioning. Control mice were provided with environmental enrichment (housing hut and bedding square) and isolated mice were housed without environmental enrichment. Isolated and group-housed controls from the same litters and were previously cage-mates prior to isolation.

Mouse surgery and general conditioning procedures were performed as described in Chapter 1. After 7 weeks of social isolation, mice underwent surgery to install a head bar for head-fixed eyelid conditioning. Following 3-5 days of recovery, mice were trained in 12 sessions (days) of weak-CS delay 400 ms ISI eyelid conditioning.

Results

Socially isolated animals learned faster and exhibited higher CR rates at plateau (Fig. 4.1) than group-housed controls. To assess how social isolation affects this form of associative learning in mice, I examined measures of learning rate and plateau performance. Learning rate was defined by the number of trials each animal needed to reach a CR rate of 25% in a sliding window of 60 trials (Fig 4.1C), and plateau performance was defined as the percentage of CRs during the final two sessions (4.1D) for all animals reaching behavioral criterion. Both groups had similar proportions of non-learners that failed to reach behavioral criterion (2/14 for controls, 0/14 for social isolation). Analysis of conditioned response properties showed no differences between the two groups (Fig. 4.2), reflecting similar cerebellar output.

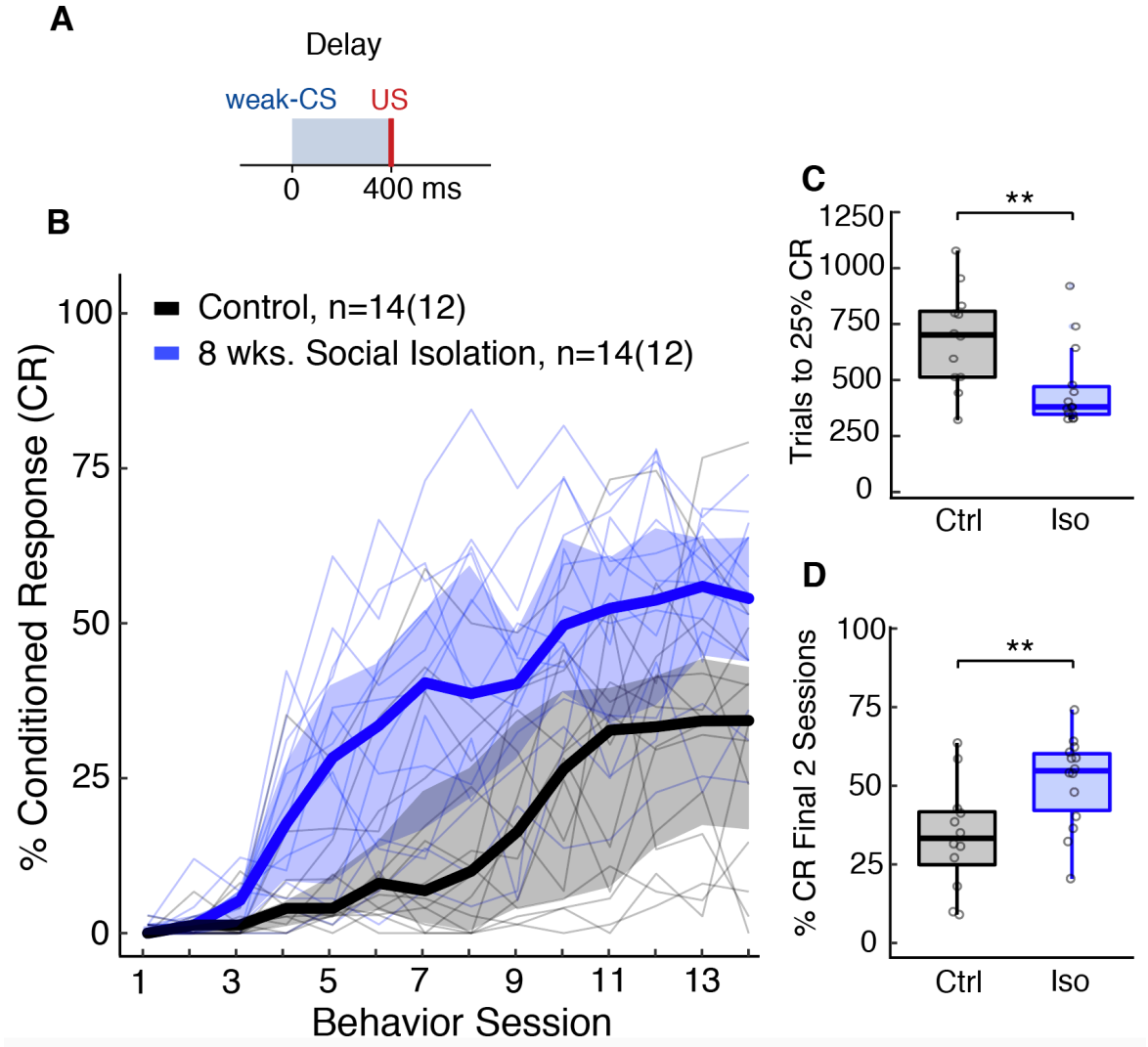

Figure 4.1: Social Isolation dramatically increases learning rate and performance

A. Stimulus configuration for delay 400 ms ISI conditioning. **B.** Learning curve over 14 days of paired training for shock (blue) and group-housed control (black) mice. Thin lines represent individual animal data, while thick lines represent group medians surrounded by shaded interquartile range of each group. Data for all animals is plotted in **A**, with number of subjects per group indicated. The adjacent number gives the number of "learners" per group, classified by achieving 25% CR over all training in a sliding window of 60 trials. **C.** Isolated mice reached learning criterion much faster than controls (avg trials to 25%CR, ctrl=684; isolation=545; Kruskal-Wallis test, stratified by sex, p=0.0082). **D.** Isolated animals also reached higher levels of CRs during the final two training sessions (avg %CR on final 2 sessions, ctrl=30%; isolation=51; Kruskal-Wallis test stratified by sex, p=.0027). Note that non-learners are excluded from **C** and **D**.

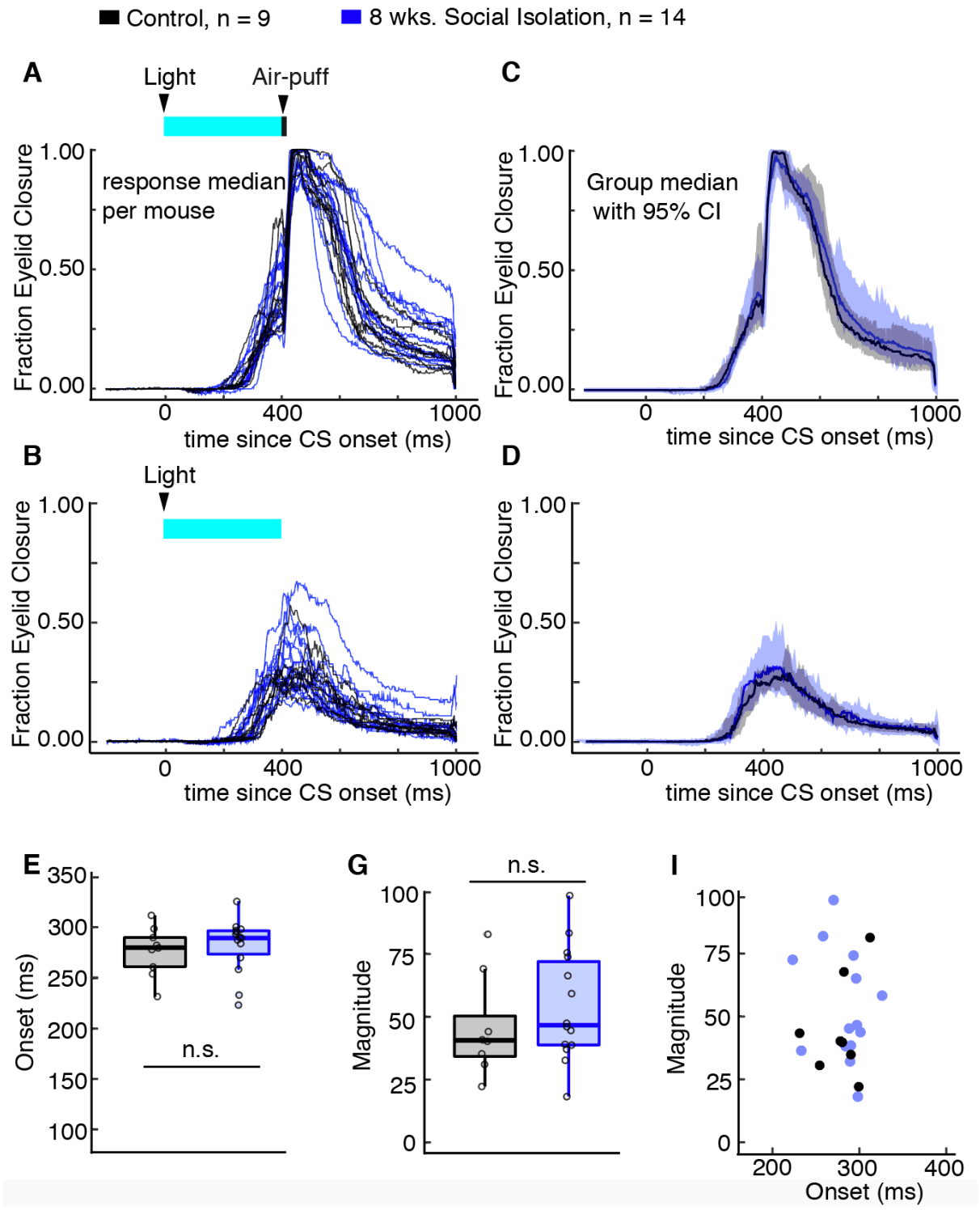

Figure 4.2: Motor response properties unchanged in in socially isolated animals.

Figure 4.2: Motor response properties unchanged in in socially isolated animals.

Socially isolated mice display conditioned response properties similar to littermates housed with mates. Single animal response medians are overlaid for paired (**A**) and probe (**C**) trials from the first 51-100 CRs made per animal. **B** and **D** depict the group-median and 95% confidence intervals of the single animal summaries in **A** and **C**. **E-F**. Kruskal Wallis tests, stratified by sex, were performed on median CR Onset ($p = 0.46$) and CR magnitude ($p = 0.60$). **G**. Two-dimensional clustering further supports similar response properties. Bright blue bar represents the time and duration of blue light CS relative to each response.

4.3 Effects of acute traumatic shock stress on eyelid conditioning

Methods

129/B6 hybrid mice of both sexes were used (n = 29; 15 females, 14 males). Mice aged 12-14 weeks at time of surgery and were counterbalanced across groups with respect to sex. Approximately one week following surgery, mice underwent shock stress, based on a stress-enhanced fear learning (SEFL) protocol developed in the laboratory of Michael Fanslow (Rajbhandari et al., 2018). This protocol was developed as a model of post-traumatic stress disorder to confer the enduring changes in learning and memory brought on by traumatic stress. Stress-induction was followed by 12 days of weak-CS delay 400 ms ISI eyelid conditioning, administered as described in Chapter 1. All behavior sessions described below took place on consecutive days across a 35-day experiment.

Following three days of mouse handling and familiarization with the experimenter, mice were placed into standard fear-conditioning chambers. Shock conditioning took place in a 30.5x24x21 cm chamber (Med Associates) with three aluminum walls, a clear Plexiglas door, and ceiling and stainless-steel grid flooring (Med-Associates VFC-005A; Context A). Conditioning chambers were contained within larger sound-attenuating chambers that were equipped with an overhead white light kept on throughout the sessions. The apparatus was cleaned between each animal with Clorox cleaning wipes and scented with 1% acetic acid solution in the waste tray below wire-grid the floor. The similar context (Context B) consisted of the same chamber with a staggered grid flooring (Med-Associates VFC-005A-S) cleaned with ethanol.

During the shock session, half of the mice (controls) freely explored the conditioning chamber for an hour. The other half (shock stress) received 10, 1 mA, 1 s un-signaled shocks that were randomly delivered (6 min PS1/WT 2 min ISI, uniform distribution) during the same one-hour session, both in Context A. Mice were transported to and from the home cage to the conditioning chamber in small white rectangle boxes.

On the day following shock, all animals underwent 3 days of rig acclimation and 2 days of rest, followed by 12 days of standard delay 400 ms ISI eyelid conditioning (75 trials per day; 60 paired, 15 probe) beginning on day 6 after shock session. After paired training, animals were presented with 2 days of CS-only extinction training (75 trials each day). On the day following the extinction sessions, mice were returned to the shock conditioning chambers, transported to and from the chambers in large gray boxes. All mice (control and shock stress) received a single shock in Context B. The purpose of this single shock session was to verify that the SEFL procedure was effective; mice that received the initial shock session before eyelid conditioning should have displayed high levels of conditioned fear (measured as freezing) upon re-exposure to Context B, indicating that the single shock was sufficient to trigger associative fear learning in the SEFL mice in Context B. Control mice did not freeze at all after a single shock in Context B, since a single shock is not sufficient to induce fear conditioning in normal, unstressed mice.

Immediately following a 5-minute context B test, during one continuous session, the shock trauma group received a second, one-hour shock session consisting of 10 more un-signaled shocks, as described above. Control mice were again allowed to freely explore the shock chamber during this same time. The following day, mice were returned to the eyelid conditioning

chambers where they underwent 8 more sessions of eyelid conditioning followed by two CS-only extinction sessions.

Results

One shock session

The differences in neurophysiology between chronic stress, such as social isolation, and acute traumatic stress, such as shock trauma, are not well-understood. Both forms of stress are known to produce general anxiety phenotypes in rodents, as well as aggression and elevated corticosterone levels. However, detailed behavioral comparison between these two forms of stress is limited. In this experiment, acute trauma shock 8 days or 1 day before behavioral testing was performed and contrasted with the previously described behavioral phenotype resulting from social isolation.

I first tested the effect of one session of acute electric shock stress on eyelid conditioning. Group median learning curve for each group showed that acute shock stress 8 days prior to training had a mild but significant effect on learning. Learning rate and performance during the final two behavior sessions were assessed. In contrast to social isolation, acute shock stress did not change how many trials required to learn the task (Fig. 4.3C; trials to 25%CR avg ctrl=551; shock=541; Kruskal-Wallis 3-group test stratified by sex, p=0.91). Indeed, they produced a higher rate of CRs late in training (Fig. 4.3D; %CR during final 2 behavior sessions avg ctrl=63%; shock=84%; Kruskal-Wallis 3-group test stratified by sex, p=0.018).

Analysis of conditioned response properties revealed a trending difference in response timing of ~30 ms, measured as shortened latency to response onset (Fig. 4.4E; CR Onset (ms) avg. ctrl=220; shock=189; Kruskal-Wallis 3-group test stratified by sex, p=0.91).

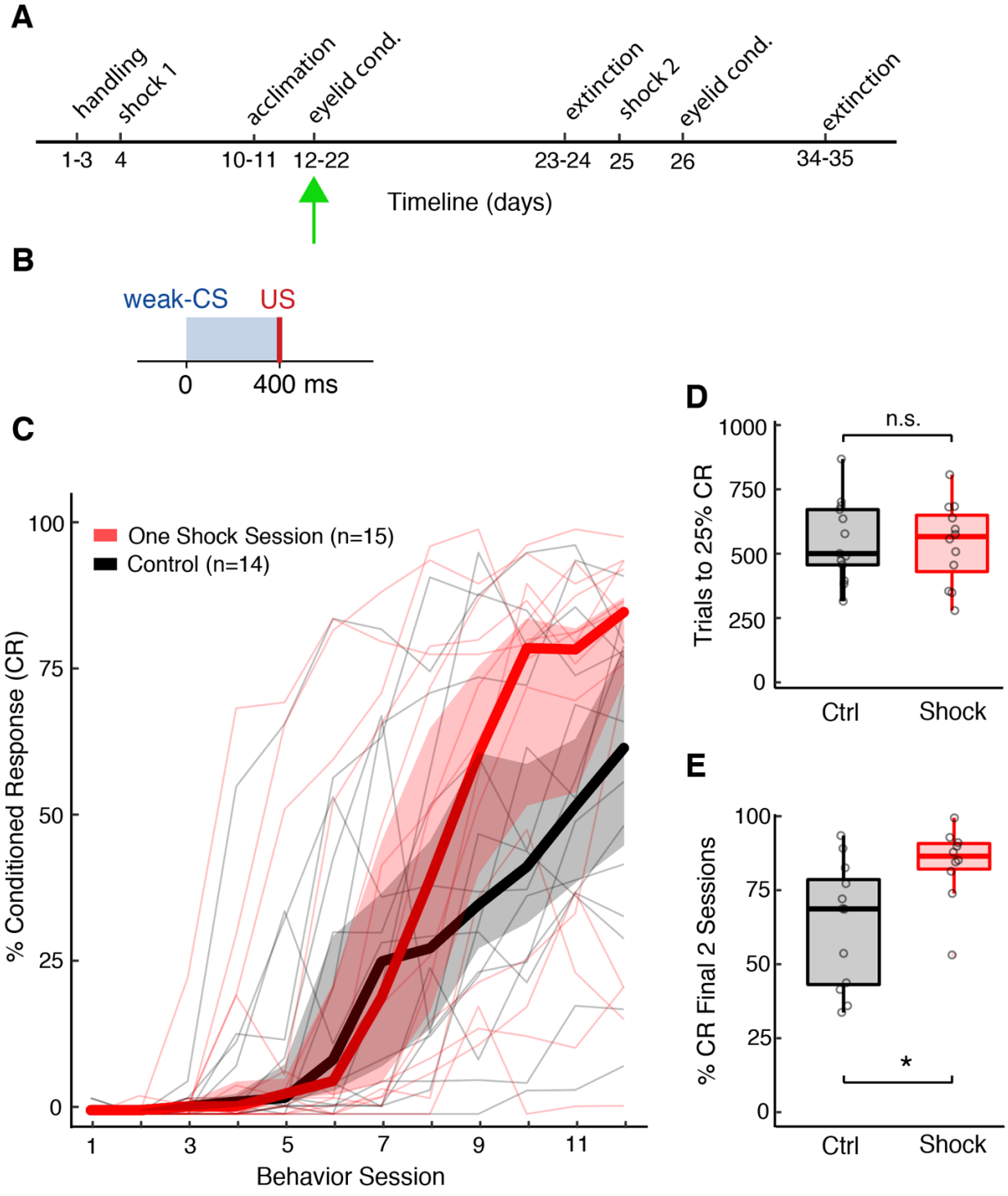

Figure 4.3: A single episode of shock stress enhances eyelid conditioning 8 days later.

Figure 4.3: A single episode of shock stress enhances eyelid conditioning 8 days later.

A. Timeline of shock stress and eyelid conditioning. Green arrow represents phase analyzed in this figure. **B.** Stimulus configuration for weak-CS delay 400 ISI conditioning. **C.** Learning curve over 12 days of paired training for shock (red) and littermate control (black) mice. Thin lines represent individual animal data, while thick lines represent group medians surrounded by shaded interquartile range of each group. Data for all animals is plotted in **B**, with number of subjects per group indicated. The adjacent number gives the number of "learners" per group, classified by achieving 25% CR over all training in a sliding window of 60 trials. **D.** Shock stress and control mice took a similar number of trails to reach learning criterion (Kruskal-Wallis test, stratified by sex, p=0.64). **E.** Shock stressed animals reached higher levels of CRs during the final two training sessions (avg %CR on final 2 sessions, ctrl=63%; isolation=84%; Kruskal-Wallis test, stratified by sex, p=0.019). Note that non-learners are excluded from **D** and **E**.

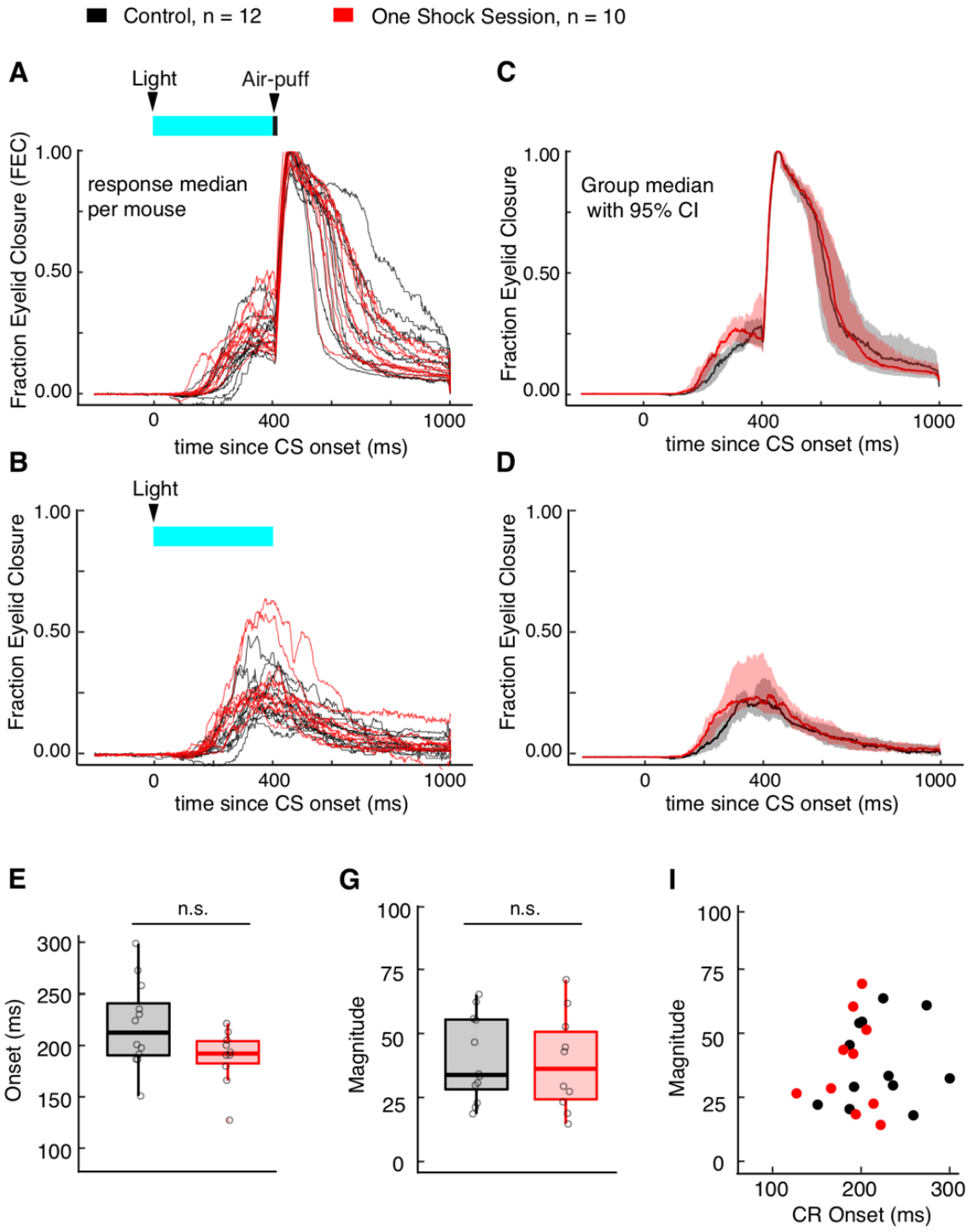

Figure 4.4: Conditioned response properties after a single session of shock stress.

Figure 4.4: Conditioned response properties after a single session of shock stress.

A single session of shock stress resulted in a trending decrease in latency to response onset. Single animal response medians are overlaid for paired (**A**) and probe (**C**) trials from the first 51-100 CRs made per animal. **B** and **D** depict the group-median and 95% confidence interval of the single animal summaries in **A** and **C**. **E-F**. Kruskal Wallis tests were performed on median CR Onset ($p=0.14$) and CR magnitude ($p=0.73$). **G**. Two-dimensional clustering visually supports the trending separation of response properties in stressed mice. Bright blue bar represents the time and duration of blue light CS relative to each response.

Two shock sessions

Immediately following two extinction sessions, previously shocked mice underwent a second round of shock trauma and again were subjected to 8 days of eyelid conditioning beginning 24 hours after the trauma. Group median learning curve, for each group showed that a second round of shock produced a similar effect on learning rate and plateau performance as only one session (Fig. 4.5C-D). That is, stressed and control mice reached behavioral criterion with a similar number of trials (Fig. 4.5C; trials to 25%CR avg ctrl=280; shock=236; Kruskal-Wallis 3-group test stratified by sex, p=0.45), but they produced a higher rate of CRs late in training (Fig. 4.5D; %CR final 2 sessions, avg ctrl=59%; shock=75%; Kruskal-Wallis 3-group test stratified by sex, p=0.011).

Analysis of conditioned response properties revealed that stressed mice produced CRs with a ~50 ms shorter onset latency (Fig. 4.6E; CR onset (ms), avg ctrl=227; shock=186; Kruskal-Wallis 3-group test stratified by sex, p=0.0084). This finding contrasts with the null effect of social isolation stress on response properties (Fig. 4.1). The strength of mossy fiber drive on cerebellar granule cells can shorten their response latency, shortening the latency to behavioral CR. Thus, a shorter response latency finding may indicate a stronger drive arriving to the cerebellum from the mossy fibers in stressed mice.

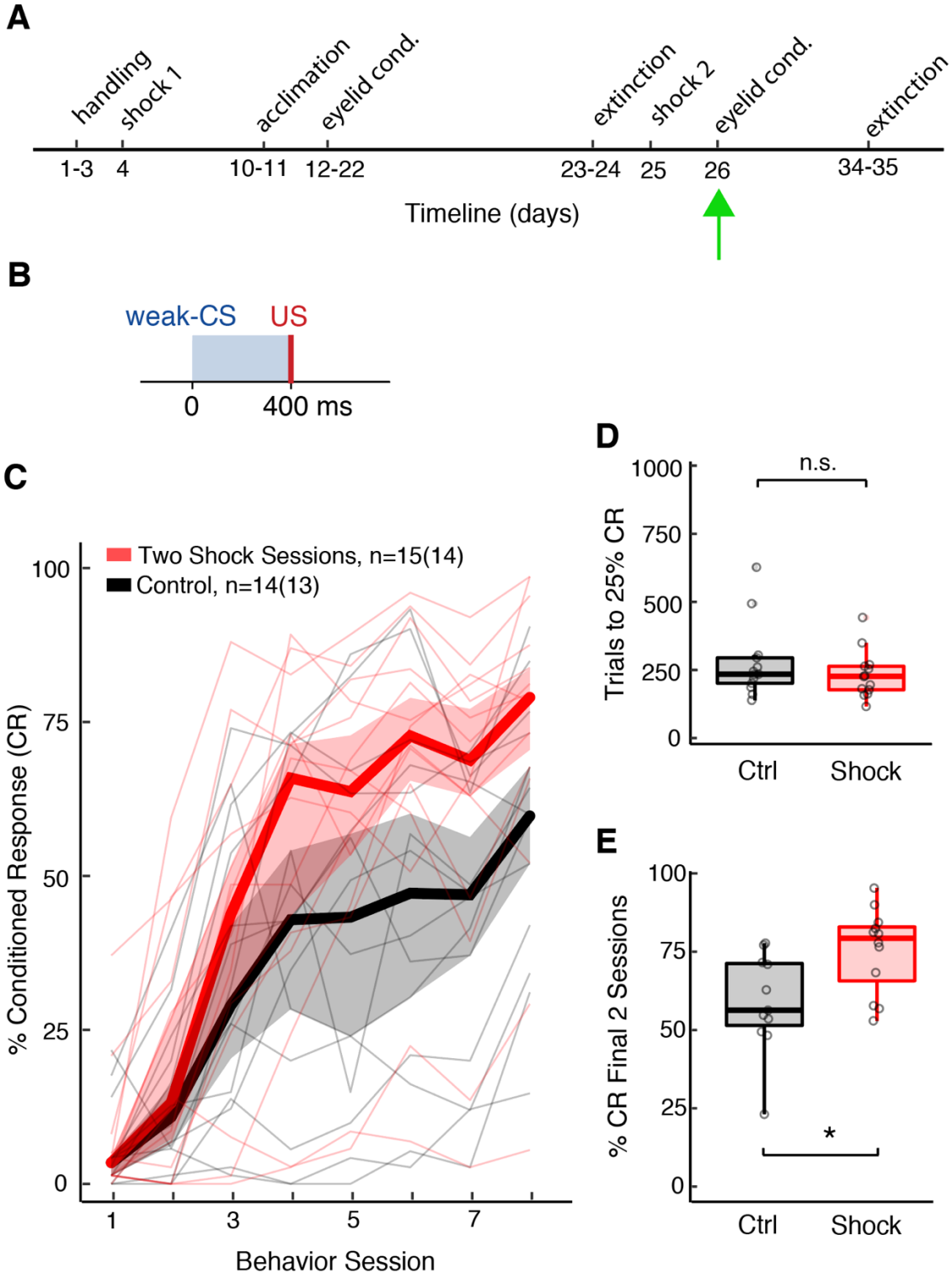

Figure 4.5: A second shock session enhances learning similarly to a single shock session

Figure 4.5: A second shock session enhances learning similarly to a single shock session

A. Timeline of shock stress and eyelid conditioning. Green arrow represents phase analyzed in this figure. **B.** Stimulus configuration for weak-CS delay 400 ISI conditioning. **C.** Learning curve over 8 days of paired training for shock (red) and littermate control (black) mice. Thin lines represent individual animal data, while thick lines represent group medians surrounded by shaded interquartile range of each group. Data for all animals is plotted in **C**, with number of subjects per group indicated. The adjacent number gives the number of "learners" per group, classified by achieving 25% CR over all training in a sliding window of 60 trials. **D.** Shock stress and control mice took similar number of trails to reach learning criterion (Kruskal-Wallis test stratified by sex, p=0.45). **E.** Shock stressed animals reached higher levels of CRs during the final two training sessions (avg %CR on final 2 sessions, ctrl=59%; isolation=75%; Kruskal-Wallis test, stratified by sex, p=0.011). Note that non-learners are excluded from **D** and **E**.

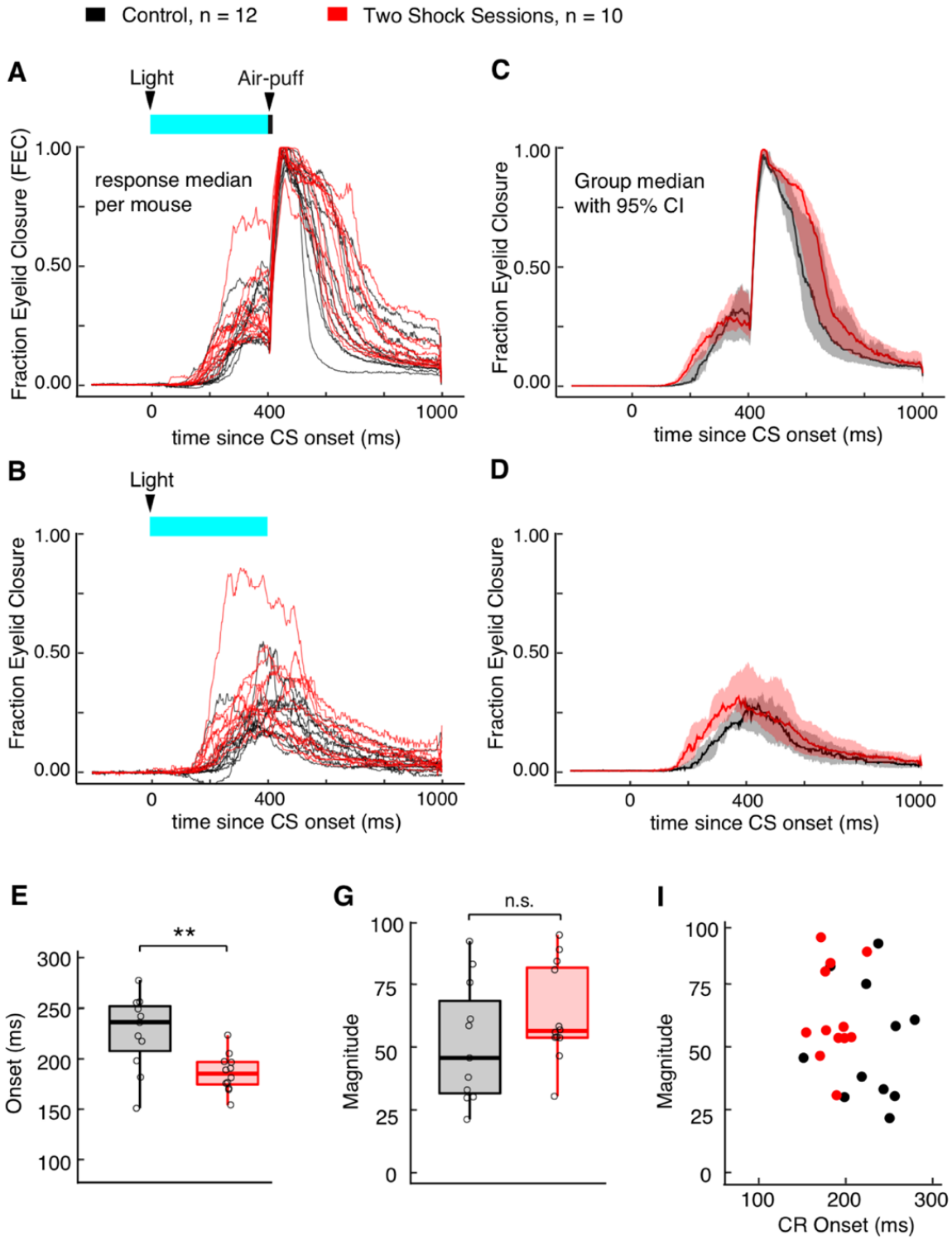

Figure 4.6: Acute shock stress induces short-latency CRs

Figure 4.6: Acute shock stress induces short-latency CRs

An additional session of shock stress resulted in ~50 ms decrease in response onset compared to non-stressed littermates. Single animal response medians are overlaid for paired (**A**) and probe (**C**) trials from the first 51-100 CRs made per animal. **B** and **D** depict the group-median and 95% confidence interval of the single animal summaries in **A** and **C**. **E-F**. Kruskal Wallis tests, stratified by sex, were performed on median CR Onset ($p=0.0066$) and CR magnitude ($p=0.26$). **G**. Two-dimensional clustering supports distinct response properties in stressed mice. Bright blue bar represents the time and duration of blue light CS relative to each response.

4.4 CONTROLLED MOSSY FIBER STIMULATION EQUALIZES LEARNING RATES IN STRESSED MICE

Methods

Male (n=13) and female (n=8) 129/B6 hybrid mice were used. For social isolation, n=10 mice (5 female) were removed from standard group housing at 6 weeks old, while n=11 (3 female) control mice remained with cage-mates. Isolated mice remained in social isolation for 10 weeks prior to the start of conditioning. Control mice were provided with environmental enrichment (housing hut and bedding square) and isolated mice were housed without environmental enrichment. Isolated and group-housed controls were from the same litters and were cage-mates prior to isolation.

For all subjects, the peripheral light CS was replaced with electrical stimulation of mossy fibers as a CS (see chapter 1 for detailed surgical and training procedures for mossy fiber stimulation). Aside from replacing the CS with direct mossy fiber stimulation, all other training procedures remained the same as described in Chapter 1 in the section on peripheral cue training.

Results

Assessment of learning rate and plateau performance revealed similar learning properties for socially isolated and group-housed mice when conditioned with direct mossy fiber stimulation (Fig. 4.7). This finding lies in sharp contrast to results described for socially isolated animals conditioned with a peripheral CS, where social isolation lead to dramatic increases in learning rate and plateau performance. When mossy fiber activation is controlled instead of

driven by CS-evoked signals processed in the forebrain, stress appears to have no effect on learning.

Finally, I examined the timing and magnitude of the conditioned responses, a measure of cerebellar-intrinsic computations (Fig. 4.8). Unexpectedly, stressed mice displayed responses that trended toward having both smaller magnitude and a longer latency to onset than control counterparts. Although neither individual measure quite reached statistical significance, two-dimensional clustering of magnitude and onset timing revealed a distinction between two populations (Fig. 4.8I).

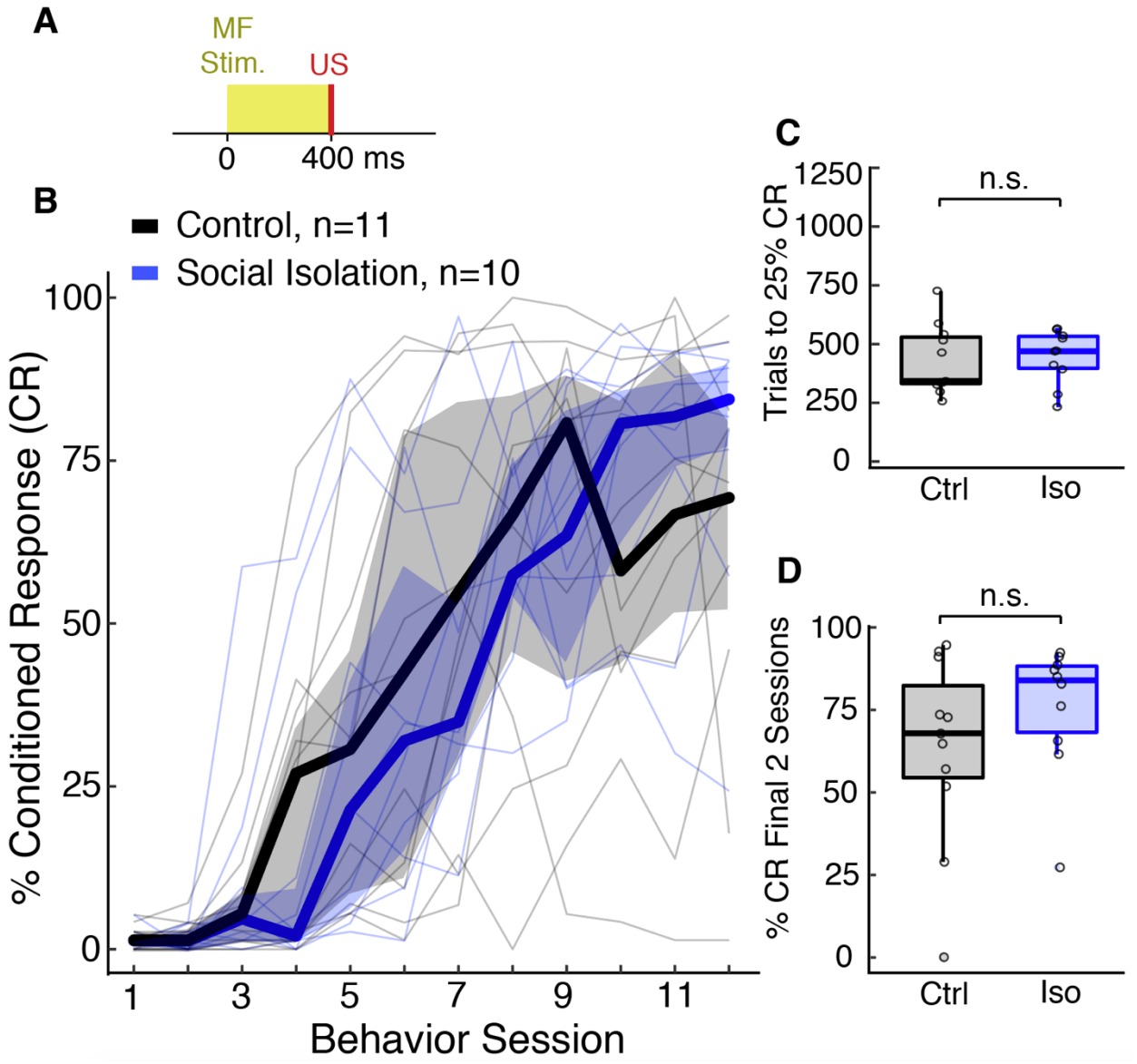

Figure 4.7: Effects of social isolation on learning disappear with mossy fiber CS.

A. Stimulus configuration for delay 400 ms ISI conditioning. **B.** Learning curve over 14 days of paired training for shock (blue) and group-housed control (black) mice. Thin lines represent individual animal data, while thick lines represent group medians surrounded by shaded interquartile range of each group. Data for all animals is plotted in **B**, with number of subjects per group indicated. No differences were detected in either **C**. learning rate (Kruskal-Wallis test stratified by sex, p=0.64) or **D.** Performance during the final two training sessions (Kruskal-Wallis test, stratified by sex, p = 0.67).

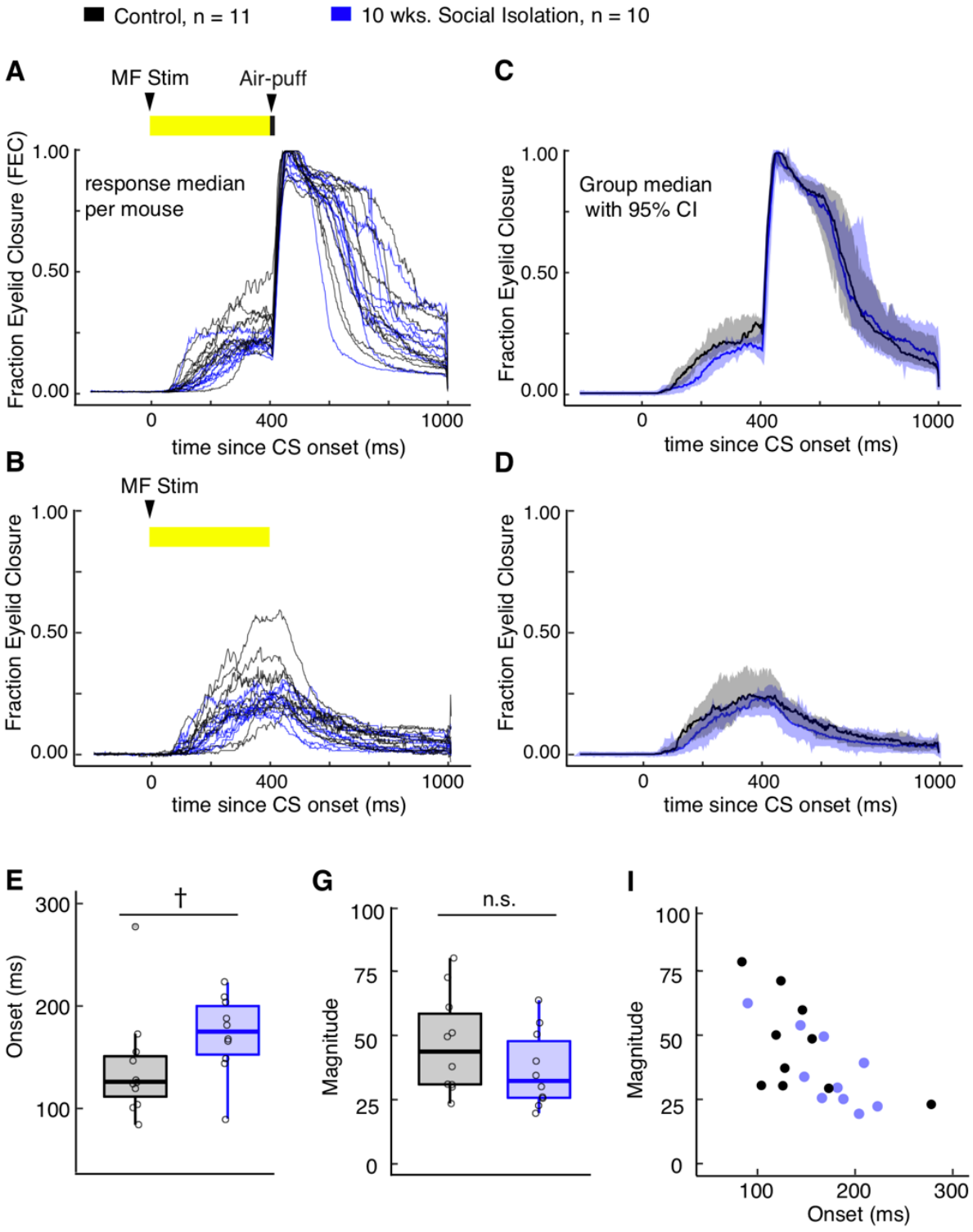

Figure 4.8: Effects of social isolation on CR properties with mossy fiber CS.

Figure 4.8: Effects of social isolation on CR properties with mossy fiber CS.

Replacing peripheral training cue with mossy fiber stimulation revealed trending ~ 50 ms delay in response onset for socially isolated mice. Single animal response medians are overlaid for paired (**A**) and probe (**C**) trials from the first 51-100 CRs made per animal. **B** and **D** depict the group-median and 95% confidence interval of the single animal summaries in **A** and **C**. **E-F**. Kruskal-Wallis test, stratified by sex, were performed on median CR Onset ($p = 0.072$) and CR magnitude ($p = 0.14$). **G**. Two-dimensional clustering shows longer latency CR onsets and smaller magnitude responses that form weak clusters. Yellow bar represents the time and duration of mossy fiber stimulation relative to each response.

4.4 DISCUSSION

Central features of stress-disorders, including PTSD and anxiety disorders, include hypersensitivity to sensory stimuli and exaggerated fears and reactions, even in the absence of threat. Eyelid conditioning is an associative learning model that seems to capture this hypersensitivity phenotype and may serve as a useful tool to disentangle the mysteries underlying circuit changes that take place in these disorders.

The effects of social isolation and acute electric shock were dissociable in two ways. First, social isolation dramatically decreased the number of trials required to reach behavioral criterion, a distinction not observed with acute shock stress. Second, shock stress altered the conditioned response timing properties, decreasing onset latency by ~50 ms as compared to non-stressed littermates.

One explanation for why these forms of stress exert distinct influence on response timing may be related to the slow timescale of social isolation stress. If stronger mossy fiber drive enhanced learning in these models, as is suggested by both forms of stress, then the cerebellum would have time to adapt to the inputs in the case of social isolation, but not necessarily in the case of acute shock trauma. When controlled mossy fiber stimulation is used to train socially isolated animals, response latency is increased by ~50 ms, and magnitude is decreased compared to non-isolated controls. Although more work is needed to understand the nature of this result, one interpretation is that the cerebellum adapts to stress-induced stronger mossy fiber inputs by reducing gain of cerebellar output. Lack of sufficient time for adaptation may help explain why acute trauma shock decreases response latency by ~50 ms to a peripheral cue while social

isolation does not change response latency, since response latency was reduced in shocked animals trained 24 hrs after shock treatment and was reduced to a lesser extent when animals were trained 8 days after shock.

Notably, a complete absence of enhanced learning in socially isolated mice with mossy fiber CS suggests that intrinsic cerebellar circuitry and climbing fiber input from the inferior olive is likely not responsible for stress-induced enhancement of conditioning. It remains to be seen if mossy fiber inputs can also account for shock-stress induced learning differences. This finding puts important constraints on the underlying mechanisms of stress-induced pathologies by demonstrating that strong mossy fiber inputs can account for enhanced learning in social isolation stress.

Chapter 5: Discussion and Conclusions

5.1 Dissociable phenotypes in two models of Alzheimer's Disease

Behavioral studies are critical to our understanding of the mechanisms underlying learning and memory. They provide information on the final output of the nervous system. Among a list of possible mechanistic explanations, behavioral experiments can narrow our focus onto which mechanisms are more likely. In chapters 2 and 3 of this dissertation, I provided novel behavioral evidence for dissociable processes in AD model mice expressing mutant PS1. These two processes were dissociable by genetic (mutant copy number) and environmental factors (stress). However, behavioral analysis alone cannot establish mechanism when the central question involves complex physiological and biochemical processes as in Alzheimer's Disease. Further work is warranted to understand how mutant PS1 interacts with stress to alter learning.

Distinguishing between putative prefrontal and amygdala origins of 3xTg and PS1 phenotypes is complicated due by the lack of basic research investigating these two putative mechanisms under normal circumstances in wild-type animals. Future research should address this problem. One experiment would entail within-animal amygdala and PFC neuronal silencing during conditioning in AD and wild-type mice. Since the prefrontal and amygdala regions important for learning and expression of trace eyelid conditioning are well-described and can be targeted with viral vectors (Siegel et al., 2017), projection-specific targeting may be possible. The end result would be a within-animal comparison PFC and amygdala contribution to eyelid conditioning in wild-type and AD mice.

5.2 Effects of stress on eyelid conditioning

Stress-sensitivity is a known feature of AD models. This feature seems to manifest in the 3xTg and PS1 models as enhanced eyelid conditioning. Because specific mechanisms leading to enhanced eyelid conditioning are poorly characterized, I endeavored to uncover the effects of two different forms of stress on eyelid conditioning in wild-type animals.

Both social isolation stress and shock stress enhance eyelid conditioning, but they do so in distinct ways. Social isolation stress increases both the rate of learning and performance after learning. Alternatively, shock stress increases performance, though it does not significantly affect learning rate. Indeed, while shock stress decreases latency to response onset, social isolation stress does not affect response timing properties. I hypothesize that this discrepancy in response timing and learning rate between the two forms of stress may be related to long-term adaptation of the cerebellum to larger CS-related cerebellar inputs resulting from stress. Further support for the cerebellar adaptation hypothesis is referenced by experiments from chapter 4 involving mossy fiber stimulation as the CS. When socially-isolated and group-housed control animals were trained with mossy fiber as the CS, the response timing of stressed animals showed signs of *increased* latency to response onset and slightly smaller magnitude response. This is what would be expected if the cerebellum were adapting to higher intensity CS inputs resulting from stress.

Ventricular infusions of the stress peptide CRF in rats have demonstrated that repeated exposure to CRF peptide (mimicking prolonged stress) can enhance eyelid conditioning (Servatius et al., 2005). Raising the possibility that the observed stress-induced changes AD models may be due, at least in part, to CRF signaling. Eyelid conditioning is well-suited to study

circuit mechanisms of CRF signaling in health and disease for three main reasons. First, since much of the circuitry involved in learning the task has been described, it is a relatively tractable circuit (Boele et al., 2009). Second, most of the brain's CRF and CRF-R1 expression is found in the cerebellum or its associated structures, such as the basilar pontine nucleus, inferior olive, and various brainstem structures contributing to the mossy fibers (Dabrowska et al., 2016, Bishop 1998), indicating this task is likely to be sensitive to CRF/ CRF1R perturbations.

5.3 THE RELATIONSHIP BETWEEN STRESS AND ALZHEIMER'S DISEASE

AD is more common in people with a history of anxiety (Petkus, et al., 2016; Pietrzak et al., 2015), depression (Ringman, et al., 2004) and PTSD (Yaffe, et al., 2010). However, the relationship between stress and AD is complicated and likely involves cross-talk between processes governing the development of AD and processes governing the stress response. One point of cross-over between the stress response and AD processes may involve signaling of the CRF peptide through the CRF-R1 receptor. The dissociable stress-related AD phenotype revealed by eyelid conditioning in this dissertation, as well as the suitability of this behavioral paradigm for studying CRF signaling mechanisms, offers opportunity for future studies with the goal of uncovering the mechanisms relating to stress and Alzheimer's Disease.

References

Ahn K, Shelton CC, Tian Y, Zhang X, Gilchrist ML, Sisodia SS, Li YM. Activation and intrinsic γ-secretase activity of presenilin 1. Proceedings of the National Academy of Sciences. 2010 Dec 14;107(50):21435-40.

Anheim M, Hannequin D, Boulay C, Martin C, Campion D, Tranchant C. Ataxic variant of Alzheimer's disease caused by Pro117Ala PSEN1 mutation. Journal of Neurology, Neurosurgery & Psychiatry. 2007 Dec 1;78(12):1414-5.

Area-Gomez E, de Groof AJ, Boldogh I, Bird TD, Gibson GE, Koehler CM, Yu WH, Duff KE, Yaffe MP, Pon LA, Schon EA. Presenilins are enriched in endoplasmic reticulum membranes associated with mitochondria. The American journal of pathology. 2009 Nov 1;175(5):1810-6.

Bao S, Chen L, Thompson RF. Classical eyeblink conditioning in two strains of mice: Conditioned responses, sensitization, and spontaneous eyeblinks. Behavioral neuroscience. 1998 Jun;112(3):714.

Beylin AV, Gandhi CC, Wood GE, Talk AC, Matzel LD, Shors TJ. The role of the hippocampus in trace conditioning: temporal discontinuity or task difficulty?. Neurobiology of learning and memory. 2001 Nov 1;76(3):447-61.

Bishop GA. Brainstem origin of corticotropin-releasing factor afferents to the nucleus interpositus anterior of the cat. Journal of chemical neuroanatomy. 1998 Sep 1;15(3):143-53.

Blankenship MR, Huckfeldt R, Steinmetz JJ, Steinmetz JE. The effects of amygdala lesions on hippocampal activity and classical eyeblink conditioning in rats. Brain research. 2005 Feb 28;1035(2):120-30.

Burriss L, Ayers E, Powell DA. Combat veterans show normal discrimination during differential trace eyeblink conditioning, but increased responsivity to the conditioned and unconditioned stimulus. Journal of psychiatric research. 2007 Nov 1;41(9):785-94.

Busche MA, Chen X, Henning HA, Reichwald J, Staufenbiel M, Sakmann B, Konnerth A. Critical role of soluble amyloid-β for early hippocampal hyperactivity in a mouse model of Alzheimer's disease. Proceedings of the National Academy of Sciences. 2012 May 29;109(22):8740-5.

Clark RF, Hutton M, Fuldner M, Froelich S, Karran E, Talbot C, Crook R, Lendon C, Prihar G, He C, Korenblat K. The structure of the presenilin 1 (S182) gene and identification of six novel mutations in early onset AD families. Nature genetics. 1995 Oct;11(2):219.

Crabbe JC, Wahlsten D, Dudek BC. Genetics of mouse behavior: interactions with laboratory environment. Science. 1999 Jun 4;284(5420):1670-2.

D'Ausilio A. Arduino: A low-cost multipurpose lab equipment. Behavior research methods. 2012 Jun 1;44(2):305-13.

De Strooper B, Annaert W, Cupers P, Saftig P, Craessaerts K, Mumm JS, Schroeter EH, Schrijvers V, Wolfe MS, Ray WJ, Goate A. A presenilin-1-dependent γ-secretase-like protease mediates release of Notch intracellular domain. Nature. 1999 Apr;398(6727):518.

Dong H, Yuede CM, Yoo HS, Martin MV, Deal C, Mace AG, Csernansky JG. Corticosterone and related receptor expression are associated with increased β-amyloid plaques in isolated Tg2576 mice. Neuroscience. 2008 Jul 31;155(1):154-63.

Edgington E, Onghena P. Randomization tests. Chapman and Hall/CRC; 2007 Feb 22.

Errico P, Barmack NH. Origins of cerebellar mossy and climbing fibers immunoreactive for corticotropin-releasing factor in the rabbit. Journal of Comparative Neurology. 1993 Oct 8;336(2):307-20.

Ezra-Nevo G, Prestori F, Locatelli F, Soda T, Michiel M, Engel M, Boele HJ, Botta L, Leshkowitz D, Ramot A, Tsoory M. Cerebellar learning properties are modulated by the CRF receptor. Journal of Neuroscience. 2018 Jul 25;38(30):6751-65.

Ezra-Nevo G, Volk N, Ramot A, Kuehne C, Tsoory M, Deussing J, Chen A. Inferior olive CRF plays a role in motor performance under challenging conditions. Translational psychiatry. 2018;8.

Farley SJ, Radley JJ, Freeman JH. Amygdala modulation of cerebellar learning. Journal of Neuroscience. 2016 Feb 17;36(7):2190-201.

Farley SJ, Albazboz H, De Corte BJ, Radley JJ, Freeman JH. Amygdala central nucleus modulation of cerebellar learning with a visual conditioned stimulus. Neurobiology of learning and memory. 2018 Apr 1;150:84-92.

Farley SJ, Radley JJ, Freeman JH. Amygdala modulation of cerebellar learning. Journal of Neuroscience. 2016 Feb 17;36(7):2190-201.

Fendt M, Koch M, Schnitzler HU. Corticotropin-releasing factor in the caudal pontine reticular nucleus mediates the expression of fear-potentiated startle in the rat. European Journal of Neuroscience. 1997 Feb;9(2):299-305.

Forsyth JK, Bolbecker AR, Mehta CS, Klaunig MJ, Steinmetz JE, O'Donnell BF, Hetrick WP. Cerebellar-dependent eyeblink conditioning deficits in schizophrenia spectrum disorders. Schizophrenia bulletin. 2010 Dec 9;38(4):751-9.

Garcia KS, Mauk MD. Pharmacological analysis of cerebellar contributions to the timing and expression of conditioned eyelid responses. Neuropharmacology. 1998 Apr 5;37(4-5):471-80.

Goate A, Chartier-Harlin MC, Mullan M, Brown J, Crawford F, Fidani L, Giuffra L, Haynes A, Irving N, James L, Mant R. Segregation of a missense mutation in the amyloid precursor protein gene with familial Alzheimer's disease. Nature. 1991 Feb;349(6311):704.

Green KN, Billings LM, Roozendaal B, McGaugh JL, LaFerla FM. Glucocorticoids increase amyloid-β and tau pathology in a mouse model of Alzheimer's disease. Journal of Neuroscience. 2006 Aug 30;26(35):9047-56.

Gruol DL, Koibuchi N, Manto M, Molinari M, Schmahmann JD, Shen Y. Essentials of cerebellum and cerebellar disorders. Springer, Berlin; 2016. Neuropeptides in the Cerebellum; p. 267-272.

Guo Q, Fu W, Sopher BL, Miller MW, Ware CB, Martin GM, Mattson MP. Increased vulnerability of hippocampal neurons to excitotoxic necrosis in presenilin-1 mutant knock-in mice. Nature medicine. 1999 Jan;5(1):101.

Guo Q, Zheng H, Justice NJ. Central CRF system perturbation in an Alzheimer's disease knockin mouse model. Neurobiology of aging. 2012 Nov 1;33(11):2678-91.

Halverson HE, Lee I, Freeman JH. Associative plasticity in the medial auditory thalamus and cerebellar interpositus nucleus during eyeblink conditioning. Journal of Neuroscience. 2010 Jun 30;30(26):8787-96.

Heiney SA, Kim J, Augustine GJ, Medina JF. Precise control of movement kinematics by optogenetic inhibition of Purkinje cell activity. Journal of Neuroscience. 2014 Feb 5;34(6):2321-30.

Heiney SA, Wohl MP, Chettih SN, Ruffolo LI, Medina JF. Cerebellar-dependent expression of motor learning during eyeblink conditioning in head-fixed mice. Journal of Neuroscience. 2014 Nov 5;34(45):14845-53.

Hothorn T, Hornik K, Van De Wiel MA, Zeileis A. Implementing a class of permutation pests: the coin package. 2008.

Johansson, Lena; Guo, Xinxin; Waern, Margda; Ostling, Svante; Gustafson, Deborah Bengtsson, Calle; Skoog, I. (2010). Midlife psychological stress and risk of dementia: a 35-year longitudinal population study. *Brain.* 2010 May 20; 133(8):2217-24.

Johnson VE, Stewart W, Smith DH. Widespread tau and amyloid-beta pathology many years after a single traumatic brain injury in humans. Brain pathology. 2012 Mar;22(2):142-9.

Jontes JD. The cadherin superfamily in neural circuit assembly. Cold Spring Harbor perspectives in biology. 2018 Jul 1;10(7):a029306.

Justice NJ, Huang L, Tian JB, Cole A, Pruski M, Hunt AJ, Flores R, Zhu MX, Arenkiel BR, Zheng H. Posttraumatic stress disorder-like induction elevates β-amyloid levels, which directly activates corticotropin-releasing factor neurons to exacerbate stress responses. Journal of Neuroscience. 2015 Feb 11;35(6):2612-23.

Kalmbach BE, Davis T, Ohyama T, Riusech F, Nores WL, Mauk MD. Cerebellar cortex contributions to the expression and timing of conditioned eyelid responses. Journal of neurophysiology. 2010 Feb 3;103(4):2039-49.

Kalmbach BE, Ohyama T, Kreider JC, Riusech F, Mauk MD. Interactions between prefrontal cortex and cerebellum revealed by trace eyelid conditioning. Learning & memory. 2009 Jan 1;16(1):86-95.

Kalmbach BE, Ohyama T, Mauk MD. Temporal patterns of inputs to cerebellum necessary and sufficient for trace eyelid conditioning. Journal of neurophysiology. 2010 May 19;104(2):627-40.

Kimoto Y, Tohyama M, Satoh K, Sakumoto T, Takahashi Y, Shimizu N. Fine structure of rat cerebellar noradrenaline terminals as visualized by potassium permanganate 'in situ perfusion'fixation method. Neuroscience. 1981 Jan 1;6(1):47-58.

Koekkoek SK, Yamaguchi K, Milojkovic BA, Dortland BR, Ruigrok TJ, Maex R, De Graaf W, Smit AE, VanderWerf F, Bakker CE, Willemsen R. Deletion of FMR1 in Purkinje cells enhances parallel fiber LTD, enlarges spines, and attenuates cerebellar eyelid conditioning in Fragile X syndrome. Neuron. 2005 Aug 4;47(3):339-52.

Kunimoto S, Nakamura S, Wada K, Inoue T. Chronic stress-mutated presenilin 1 gene interaction perturbs neurogenesis and accelerates neurodegeneration. Experimental neurology. 2010 Jan 1;221(1):175-85.

Kuzuya A, Zoltowska KM, Post KL, Arimon M, Li X, Svirsky S, Maesako M, Muzikansky A, Gautam V, Kovacs D, Hyman BT. Identification of the novel activity-driven interaction between synaptotagmin 1 and presenilin 1 links calcium, synapse, and amyloid beta. BMC biology. 2016 Dec;14(1):25.

Lemere CA, Lopera F, Kosik KS, Lendon CL, Ossa J, Saido TC, Yamaguchi H, Ruiz A, Martinez A, Madrigal L, Hincapie L. The E280A presenilin 1 Alzheimer mutation produces increased Aβ42 deposition and severe cerebellar pathology. Nature medicine. 1996 Oct;2(10):1146.

Manns JR, Clark RE, Squire LR. Awareness predicts the magnitude of single-cue trace eyeblink conditioning. Hippocampus. 2000;10(2):181-6.

Marambaud P, Wen PH, Dutt A, Shioi J, Takashima A, Siman R, Robakis NK. A CBP binding transcriptional repressor produced by the PS1/ϵ-cleavage of N-cadherin is inhibited by PS1 FAD mutations. Cell. 2003 Sep 5;114(5):635-45.

Mauk MD, Steinmetz JE, Thompson RF (1986) Classical conditioning using stimulation of the inferior olive as the unconditioned stimulus. Proc Natl Acad Sci U S A 83:5349–5353.

Meckler X, Checler F. Presenilin 1 and presenilin 2 target γ-secretase complexes to distinct cellular compartments. Journal of Biological Chemistry. 2016 Jun 10;291(24):12821-37.

Meckler X, Checler F. Visualization of specific γ-secretase complexes using bimolecular fluorescence complementation. Journal of Alzheimer's Disease. 2014 Jan 1;40(1):161-76.

Miyata M, Okada D, Hashimoto K, Kano M, Ito M. Corticotropin-releasing factor plays a permissive role in cerebellar long-term depression. Neuron. 1999 Apr 1;22(4):763-75.

Mohamed AZ, Cumming P, Srour H, Gunasena T, Uchida A, Haller CN, Nasrallah F, Department of Defense Alzheimer's Disease Neuroimaging Initiative. Amyloid pathology fingerprint differentiates post-traumatic stress disorder and traumatic brain injury. Neuroimage: clinical. 2018 Jan 1;19:716-26.

Moyer, J. R., Jr., Deyo, R. A., & Disterhoft, J. F. (1990). Hippocampectomy disrupts trace eye-blink conditioning in rabbits. Behavioral Neuroscience, 104, 243–252.

Mullane K, Williams M. Alzheimer's disease (AD) therapeutics-1: Repeated clinical failures continue to question the amyloid hypothesis of AD and the current understanding of AD causality. Biochemical pharmacology. 2018 Sep 29.

Myers CE, VanMeenen KM, Devin McAuley J, Beck KD, Pang KC, Servatius RJ. Behaviorally inhibited temperament is associated with severity of post-traumatic stress disorder symptoms and faster eyeblink conditioning in veterans. Stress. 2012 Jan 1;15(1):31-44.

Park HJ, Ran Y, Jung JI, Holmes O, Price AR, Smithson L, Ceballos-Diaz C, Han C, Wolfe MS, Daaka Y, Ryabinin AE. The stress response neuropeptide CRF increases amyloid-β

production by regulating γ-secretase activity. The EMBO journal. 2015 Jun 12;34(12):1674-86.

Petkus, Andrew J., et al. "Anxiety is associated with increased risk of dementia in older Swedish twins." *Alzheimer's & Dementia* 12.4 (2016): 399-406.

Pibiri F, Nelson M, Guidotti A, Costa E, Pinna G. Decreased corticolimbic allopregnanolone expression during social isolation enhances contextual fear: a model relevant for posttraumatic stress disorder. Proceedings of the National Academy of Sciences. 2008 Apr 8;105(14):5567-72.

Pietrzak, Robert H., et al. "Amyloid-β, anxiety, and cognitive decline in preclinical Alzheimer disease: A multicenter, prospective cohort study." *Jama psychiatry* 72.3 (2015): 284-291.

Pochiro JM, Lindquist DH. Central amygdala lesions inhibit pontine nuclei acoustic reactivity and retard delay eyeblink conditioning acquisition in adult rats. Learning & behavior. 2016 Jun 1;44(2):191-201.

Pomrenze MB, Millan EZ, Hopf FW, Keiflin R, Maiya R, Blasio A, Dadgar J, Kharazia V, De Guglielmo G, Crawford E, Janak PH. A transgenic rat for investigating the anatomy and function of corticotrophin releasing factor circuits. Frontiers in neuroscience. 2015 Dec 24;9:487.

Poulin, Stéphane P., et al. "Amygdala atrophy is prominent in early Alzheimer's disease and relates to symptom severity." *Psychiatry Research: Neuroimaging* 194.1 (2011): 7-13.

Quiroz YT, Willment KC, Castrillon G, Muniz M, Lopera F, Budson A, Stern CE. Successful scene encoding in presymptomatic early-onset Alzheimer's disease. Journal of Alzheimer's Disease. 2015 Jan 1;47(4):955-64.

Rajbhandari AK, Gonzalez ST, Fanselow MS. Stress-enhanced fear learning, a robust rodent model of post-traumatic stress disorder. JoVE (Journal of Visualized Experiments). 2018 Oct 13(140):e58306.

R Core Team (2019). R: A language and environment for statistical computing. R Foundation for Statistical Computing, Vienna, Austria. URL https://www.R-project.org/.

Rothman SM, Herdener N, Camandola S, Texel SJ, Mughal MR, Cong WN, Martin B, Mattson MP. 3xTgAD mice exhibit altered behavior and elevated Aβ after chronic mild social stress. Neurobiology of aging. 2012 Apr 1;33(4):830-e1.

Rosen, J. B., & Davis, M. (1988). Enhancement of Acoustic Startle by Electrical Stimulation of the Amygdala. *Behavioral Neuroscience*, *102*(2), 195–202.

Ryman DC, Acosta-Baena N, Aisen PS, Bird T, Danek A, Fox NC, Goate A, Frommelt P, Ghetti B, Langbaum JB, Lopera F. Symptom onset in autosomal dominant Alzheimer disease: a systematic review and meta-analysis. Neurology. 2014 Jul 15;83(3):253-60.

Sears LL, Finn PR, Steinmetz JE. Abnormal classical eye-blink conditioning in autism. Journal of autism and developmental disorders. 1994 Dec 1;24(6):737-51.

Schedin-Weiss S, Caesar I, Winblad B, Blom H, Tjernberg LO. Super-resolution microscopy reveals γ-secretase at both sides of the neuronal synapse. Acta neuropathologica communications. 2016 Dec;4(1):29.

Shen L, Qin W, Wu L, Zhou A, Tang Y, Wang Q, Jia L, Jia J. Two novel presenilin-1 mutations (I249L and P433S) in early onset Chinese Alzheimer's pedigrees and their functional characterization. Biochemical and Biophysical Research Communications. 2019 Jun 21.

Sherrington R, Froelich S, Sorbi S, Campion D, Chi H, Rogaeva EA, Levesque G, Rogaev EI, Lin C, Liang Y, Ikeda M. Alzheimer's disease associated with mutations in presenilin 2 is rare and variably penetrant. Human molecular genetics. 1996 Jul 1;5(7):985-8.

Shors TJ, Weiss C, Thompson RF. Stress-induced facilitation of classical conditioning. Science. 1992 Jul 24;257(5069):537-9.

Siegel JJ, Taylor W, Gray R, Kalmbach B, Zemelman BV, Desai NS, Johnston D, Chitwood RA. Trace eyeblink conditioning in mice is dependent upon the dorsal medial prefrontal cortex, cerebellum, and amygdala: behavioral characterization and functional circuitry. Eneuro. 2015 Jul;2(4).

Servatius RJ, Beck KD, Moldow RL, Salameh G, Tumminello TP, Short KR. A stress-induced anxious state in male rats: corticotropin-releasing hormone induces persistent changes in associative learning and startle reactivity. Biological psychiatry. 2005 Apr 15;57(8):865-72.

Steinmetz AB, Ng KH, Freeman JH. Memory consolidation within the central amygdala is not necessary for modulation of cerebellar learning. Learning & Memory. 2017 Jun 1;24(6):225-30.

Steinmetz JE, Lavond DG, Thompson RF (1985) Classical conditioning of the rabbit eyelid response with mossy fiber stimulation as the conditioned stimulus. Bull Psychon Soc 23:245–248.

Steinmetz JE, Lavond DG, Thompson RF (1989) Classical conditioning in rabbits using pontine nucleus stimulation as a conditioned stimulus and inferior olive stimulation as an unconditioned stimulus. Synapse 3:225–233.

Steinmetz JE, Rosen DJ, Chapman PF, Lavond DG, Thompson RF (1986) Classical conditioning of the rabbit eyelid response with a mossy-fiber stimulation CS: I. Pontine nuclei and middle cerebellar peduncle stimulation. Behav Neurosci 100:878–887.

Stevens LM, Brown RE. Reference and working memory deficits in the 3xTg-AD mouse between 2 and 15-months of age: a cross-sectional study. Behavioural brain research. 2015 Feb 1;278:496-505.

Stover KR, Campbell MA, Van Winssen CM, Brown RE. Early detection of cognitive deficits in the 3xTg-AD mouse model of Alzheimer's disease. Behavioural brain research. 2015 Aug 1;289:29-38.

Stuart, Kimberley E., et al. "Environmental novelty exacerbates stress hormones and Aβ pathology in an Alzheimer's model." *Scientific Reports* 7.1 (2017): 2764.

Stutzmann GE, Caccamo A, LaFerla FM, Parker I. Dysregulated IP3 signaling in cortical neurons of knock-in mice expressing an Alzheimer's-linked mutation in presenilin1 results in exaggerated Ca2+ signals and altered membrane excitability. Journal of Neuroscience. 2004 Jan 14;24(2):508-13.

Sun X, Beglopoulos V, Mattson MP, Shen J. Hippocampal spatial memory impairments caused by the familial Alzheimer's disease-linked presenilin 1 M146V mutation. Neurodegenerative Diseases. 2005;2(1):6-15.

Takehara K, Kawahara S, Takatsuki K, Kirino Y. Time-limited role of the hippocampus in the memory for trace eyeblink conditioning in mice. Brain research. 2002 Oct 4;951(2):183-90.

Tanzi RE. The genetics of Alzheimer disease. Cold Spring Harbor perspectives in medicine. 2012 Oct 1;2(10):a006296.

Thompson RF. In search of memory traces. Annu. Rev. Psychol.. 2005 Feb 4;56:1-23.

Walker DL, Davis M. Double dissociation between the involvement of the bed nucleus of the stria terminalis and the central nucleus of the amygdala in startle increases produced by conditioned versus unconditioned fear. Journal of Neuroscience. 1997 Dec 1;17(23):9375-83.

Wang Y, Chen ZP, Zhuang QX, Zhang XY, Li HZ, Wang JJ, Zhu JN. Role of corticotropin-releasing factor in cerebellar motor control and ataxia. Current Biology. 2017 Sep 11;27(17):2661-9.

Wang R, Dineley KT, Sweatt JD, Zheng H. Presenilin 1 familial Alzheimer's disease mutation leads to defective associative learning and impaired adult neurogenesis. Neuroscience. 2004 Jan 1;126(2):305-12.

Weiss, C., Sametsky, E., Sasse, A., Spiess, J., & Disterhoft, J. F. (2005). Acute stress facilitates trace eyeblink conditioning in C57BL/6 male mice and increases the excitability of their CA1 pyramidal neurons. *Learning & Memory*.

Welsh JP, Oristaglio JT. autism and classical eyeblink conditioning: Performance changes of the conditioned response related to autism spectrum Disorder Diagnosis. Frontiers in psychiatry. 2016 Aug 11;7:137.

Wu GY, Liu SL, Yao J, Sun L, Wu B, Yang Y, Li X, Sun QQ, Feng H, Sui JF. Medial Prefrontal Cortex–Pontine Nuclei Projections Modulate Suboptimal Cue-Induced Associative Motor Learning. Cerebral cortex. 2017 Jan 11;28(3):880-93.

Yaffe, K., Vittinghoff, E., Lindquist, K., Barnes, D., Covinsky, K. E., Neylan, T., … Marmar, C. (2010). Posttraumatic Stress Disorder and Risk of Dementia Among US Veterans. *Arch Gen Psychiatry*, *67*(6), 608–613.

Zhang C, Wu B, Beglopoulos V, Wines-Samuelson M, Zhang D, Dragatsis I, Südhof TC, Shen J. Presenilins are essential for regulating neurotransmitter release. Nature. 2009 Jul;460(7255):632.

Zhang C, Kuo CC, Moghadam SH, Monte L, Campbell SN, Rice KC, Sawchenko PE, Masliah E, Rissman RA. Corticotropin- releasing factor receptor-1 antagonism mitigates beta amyloid pathology and cognitive and synaptic deficits in a mouse model of Alzheimer's disease. Alzheimer's & Dementia. 2016 May 1;12(5):527-37.

Zhang C, Wu B, Beglopoulos V, Wines-Samuelson M, Zhang D, Dragatsis I, Südhof TC, Shen J. Presenilins are essential for regulating neurotransmitter release. Nature. 2009 Jul;460(7255):632.

Zoltowska KM, Maesako M, Lushnikova I, Takeda S, Keller LJ, Skibo G, Hyman BT, Berezovska O. Dynamic presenilin 1 and synaptotagmin 1 interaction modulates exocytosis and amyloid β production. Molecular neurodegeneration. 2017 Dec;12(1):15.

Vita

Cheasequah Jolene Blevins was born in Columbus, Ohio to parents Sharon Marcum and Jetto Blevins. She graduated from Northridge High School in Johnstown, Ohio in May of 2006 before enrolling at Ohio State University that fall. Cheasequah graduated from Ohio State in May 2011 with a Bachelor of Science in molecular genetics and minors in mathematics and Spanish. She then spent a year as a Fulbright Fellow in Barcelona, Spain before enrolling in concurrent Neuroscience (Ph.D.) and Statistics (M.S.) programs at the University of Texas at Austin in fall of 2013 to pursue her interests in the biology of learning and memory.

Permanent email address: cheasequah.blevins@gmail.com

This dissertation was typed by the author.